嘉南藥理科技大學專題研究計畫成果報告

計畫編號：CNIC-98-01

計畫名稱：類薑黃素對草菇酪胺酸酶活性及 B16 細胞之黑色素形成之影響

執行期間：98 年 1 月 1 日至 98 年 12 月 31 日

■整合型計畫	□個別型計畫
計畫總主持人：楊朝成	計畫主持人：
子計畫主持人：楊朝成、郭玫君	
子計畫共同主持人：郭玫君	
計畫參與人員：楊朝成、郭玫君、吳明娟、張綺芳、蔡幸芳、黃郁媛和吳婉君	

中華民國 99 年 02 月 28 日

摘要

薑黃(*Curcuma longa* Linn)是一種薑科植物，其根狀地下莖萃取出主要成份為薑黃素 (Curcumin)、去甲氧基薑黃素(Demethoxycurcumin)、去二甲氧基薑黃素(Bidemethoxycurcumin)，合稱為類薑黃素(Curcuminoids)；另外四氫薑黃素(Tetra-hydro curcumin)則是薑黃素之代謝產物。本研究之目的為探討類薑黃素是否可藉由抑制酪胺酸酶的活性而降低黑色素的生合成，以及其抑制機轉。

本研究將類薑黃素加入酪胺酸酶與不同的酵素基質(tyrosine或L-DOPA)共同作用，其後偵測490㎚吸光值以及檢測其有效抑制酪胺酸酶活性百分之五十的濃度(IC_{50})；結果顯示Curcumin、Demethoxycurcumin、Bidemethoxycurcumin和Tetra-hydro curcumin，其IC_{50}(tyrosine)分別為：71.83、14.14、8.65和54.33μM，其中以Bidemethoxycurcumin抑制效果最佳。再者研究其抑制酵素活性之機制，利用基質和反應速率進行Lineweaver-Burk plots雙倒數作圖以判定抑制酵素的形態，結果發現其均為競爭型的抑制。進一步將化合物進行B16的細胞測試，結果發現20㎛ Demethoxycurcumin、Bidemethoxycurcumin和curcumin作用72小時後，黑色素含量減少，且細胞存活率達80%以上。

未來希望可將化合物進行相關動物試驗，以期拓展類薑黃素在黑色素抑制劑之應用價值。

關鍵字：類薑黃素、酪胺酸酶、IC_{50}、B16 細胞

前言

黑色素廣泛分布在動物、植物和微生物內，其能阻擋紫外線的穿透使真皮及皮下組織免受紫外線的傷害。不過黑色素的過度產生，會在皮膚上產生黃褐斑、黑斑及皮膚癌。美白治劑添加於多種保養品和化粧品中，為了使消費者使用後不致產生副作用，其除了具美白功效外，還必須兼具穩定性及安全性，於是安全無毒性的美白治劑並成了目前的新趨勢。天然萃取物相對於化學合成物，其穩定性高且較易被生物體吸收和代謝，因此是一絕佳的選擇。另外蔬果及菇蕈類的褐變也和黑色素有關；農產品的褐變直接影響外觀，進而降低售價。黑色素的生合成又與酪胺酸酶和其相關蛋白質的活性相關。因此抑制酪胺酸酶及其相關蛋白質的活性，便可阻斷黑色素的生合成。

本研究主要利用類薑黃素來探討其抑制酪胺酸酶的活性，以及抑制的機轉。並利用B16小鼠黑色素瘤細胞株，來探討樹蕃茄萃取物對於抑制胞內酪胺酸酶及其相關蛋白質的活性。期望此種天然物可用於人類美白治劑或防止蔬果核變，進而經過相關動物試驗甚至於臨床試驗，爾後能夠應用於醫療美白或降低農產品褐變之用。

結果和討論

黑色素之生合成是由酪胺酸酶催化酪胺酸形成 L-DOPA，L-DOPA 再經由酪胺酸酶催化形成黑色素。將不同濃度的 curcumin、Demethoxycurcumin、Bisdemethoxy- curcumin、Tetra-hydro curcumin 四種化合物，以及 Kojic acid(正對照組以草菇酪胺酸酶和不同的酵素基質(L-Tyrosine 或 L-DOPA)共同作用，再偵測其作用溶液的吸光值來推斷類薑黃素抑制酪胺酸酶活性達百分之五十之濃度。其結果如表 1 所示，Bisde-methoxycurcumin 抑制效果最佳，在低濃度 8.65±0.43 μM即可降低百分之五十的草菇酪胺酸酶活性；Demethoxycurcumin 次之 IC50 為 14.14±1.27 μM； Bisdemethoxycurcumin 和 Demethoxycurcumin 兩者 IC50 皆優於正對照組的 Kojic acid (20.86±2.62 μM)。另外 Curcumin 和 Tetra-hydro curcumin 也具有抑制草菇酪胺酸酶的能力，其 IC50 分別為 71.83±3.68 μM和 54.33±0.17 μM。而抑制草菇酪胺酸酶活性形成多巴的 IC50 結果如表 2 所示：其中以 Bisdemethoxycurcumin 效果為最佳，IC50 達 9.89±3.01 μM，效果遠比 Kojic acid 之 42.59±5.37 μM為佳；Demethoxycurcumin 之 IC50 為 56.72±1.11 μM，其餘二個化合物之 IC50 皆大於 100 μM。

表 1 類薑黃素純化合物以酪胺酸(Tyrosine)為反應基質下抑制酪胺酸酶活性的能力

Compound	IC50 [a] (μ M) of L-Tyrosine ± SD
Curcumin	71.83±3.68
Demethoxycurcumin	14.14±1.27
Bisdemethoxycurcumin	8.65±0.43
Tetra-hydro curcumin	54.33±0.17
Kojic acid	20.86±2.62

[a]IC50:是可以抑制酪胺酸酶活性達百分之五十的樣品濃度

表 2 類薑黃素純化合物分別在以 L-DOPA 為反應基質下抑制酪胺酸酶活性的能力

Compound	IC50 [a] (μ M) of L-DOPA ± SD
Curcumin	>100
Demethoxycurcumin	56.72±1.11
Bisdemethoxycurcumin	9.89±3.01
Tetra-hydro curcumin	>100
Kojic acid	42.59±5.37

[a]IC50:是可以抑制酪胺酸酶活性達百分之五十的樣品濃度

再者研究其抑制酵素活性之機制，以 0 μ M、8 μ M 和 12 μ M 的酪胺酸和酪胺酸酶共同作用，並偵測其反應速率，利用基質濃度和反應速率，以 Lineweaver-Burk plots 作圖並計算 Vmax 和 Km。四種試驗化合物結果由圖 1 顯示，不同濃度抑制物之作用線皆相交於 Y 軸，顯示其 Vmax 相同，其皆為競爭型抑制。另外由表 3 可看出 Bisdemethoxycurcumin 之 Km (0.727mM)最高，其次為 Demethoxycurcumin (0.712mM)、Curcumin (0.654mM)，最後為 Tetra-hydro curcumin (0.479mM)，其皆高於對照組的 0.338mM。此結果顯示類薑黃素與酪胺酸競爭酪胺酸酶的結合位置，因此抑制酪胺酸酶的活性。

表 3 類薑黃素(a)Curcumin,(b)DMC,(c)BDMC,(d)THC 酪胺酸酶抑制型態及活性動力參數(Vmax,Km)之影響

Compound	抑制形式 [a]	Km(mM)	Vmax(△OD490/min)
Normal	/	0.338	0.067
Curcumin	Competitive	0.654	0.068
Demethoxycurcumin	Competitive	0.712	0.071
Bisdemethoxycurcumin	Competitive	0.727	0.068
Tetra-hydro curcumin	Competitive	0.479	0.067

[a] 酪胺酸酶與基質酪胺酸反應的結果

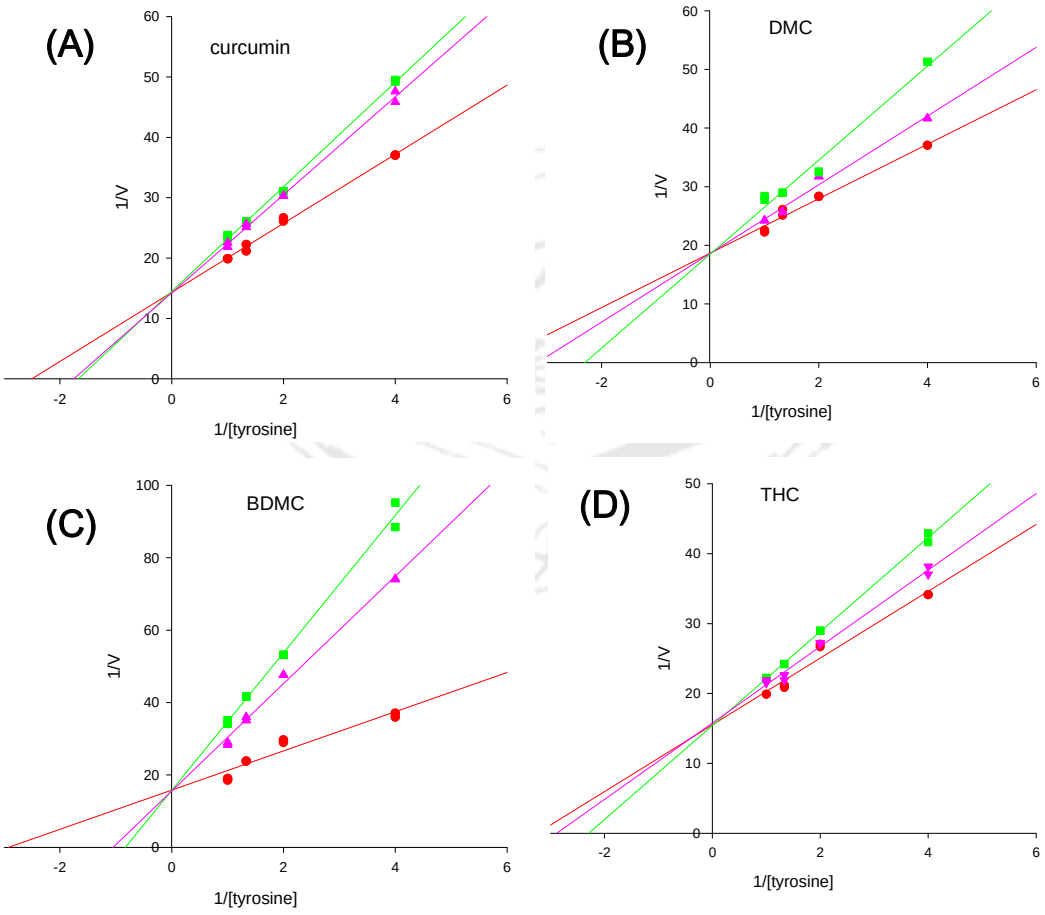

圖 1 (a)Curcumin，(b)DMC，(c)BDMC，(d)THC 以酪胺酸為基質抑制酪胺酸酶之雙倒數圖

最後我們將化合物進行小鼠黑色素瘤細胞 B16 F10的細胞測試，經MTT測試

在20mM的類薑黃素處理下，B16細胞的存活率多為80%以上，統計上與空白組並無顯著差異(如圖2所示)。另外在抑制B16細胞產生黑色素實驗中，結果顯示(圖 3) 20μM Demethoxycurcumin、Bidemethoxycurcumin和curcumin作用72小時後，B16細胞之黑色素驟減至20%以下(p<0.01)。

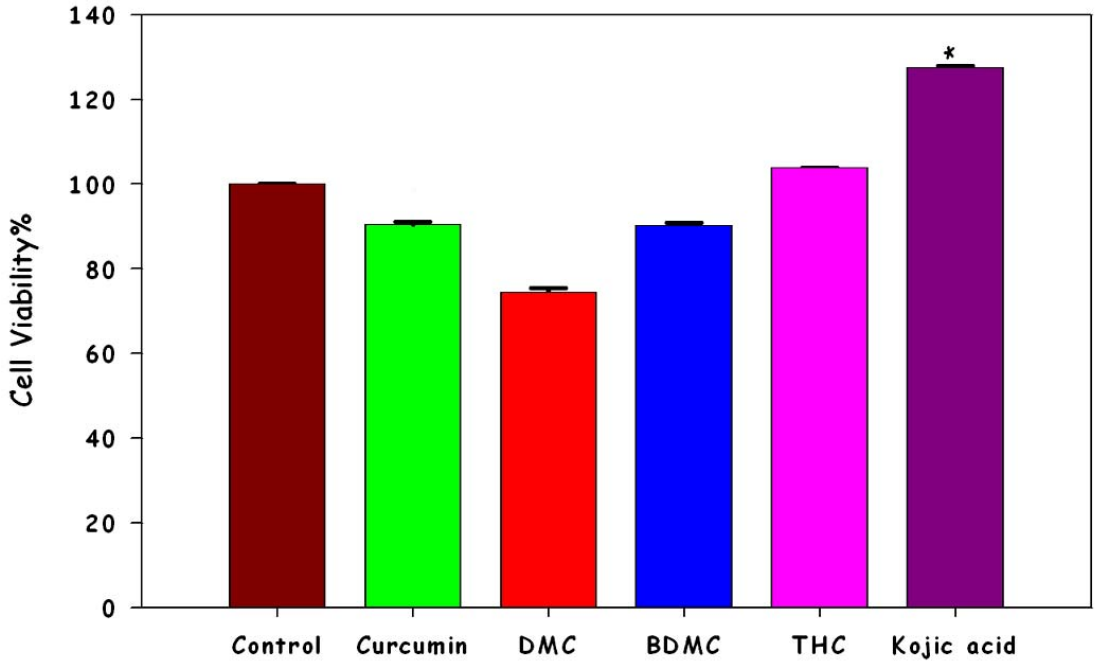

圖 2. 類薑黃素在黑色素腫瘤細胞上的細胞毒性測試。

(＊P-value<0.05 ， ＊＊ P-value<0.01)

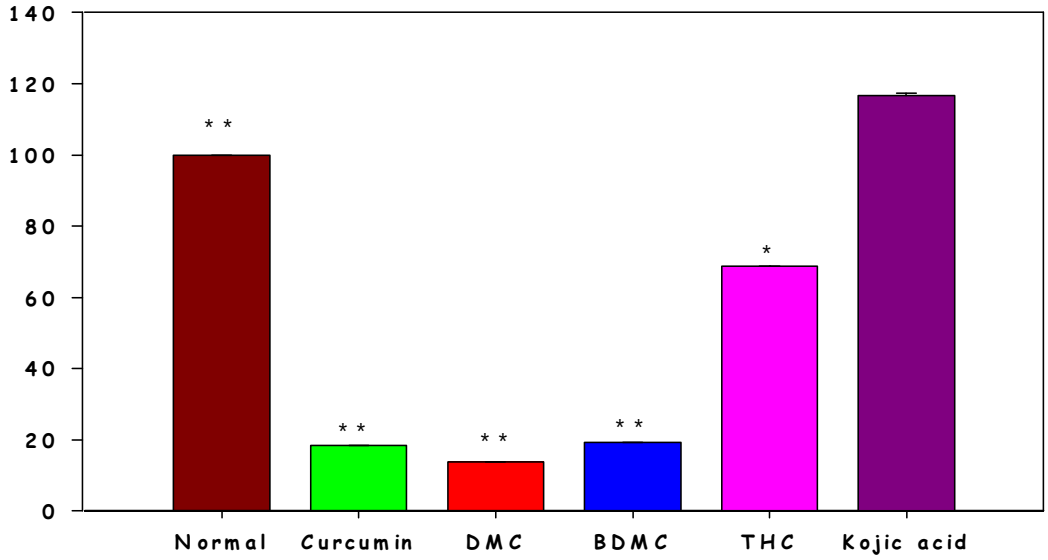

圖 3. 類薑黃素對 B16 細胞胞內黑色素含量之影響。

（＊P-value<0.05 ， ＊＊ P-value<0.01）

酚類物質相關產品目前已廣泛使用於日常生活；有許多文獻指出，植物中所含的酚類化合物能有效抗氧化、清除自由基。除此之外，亦有文獻說明酚類化合物因結構上的特性，能與基質競爭酪胺酸酶而達到抑制酪胺酸酶活性的效果。本研究以結構上屬多酚類化合物的類薑黃素研究其抑制草菇酪胺酸活性，結果發現類薑黃素多能有效抑制草菇酪胺酸酶的活性。由於此些化合物部分結構與酪胺酸相似，因此其皆與基質競爭酵素活性之鍵結區而達到降低酵素活性之目的。在 B16 的細胞測試中，也有極佳地抑制黑色素的功效，未來希望可深入探討抑制胞內黑色素生合成的機轉及進行相關動物試驗，以期拓展類薑黃素在黑色素抑制劑之應用價值。

謝誌

感謝嘉南藥理科技大學的經費支持，另外感謝美國Rutgers(the state university of New Jersey) 食品科學系何其檉教授提供類薑黃素純化合物。

參考文獻

[1] Arslan O., E. M., Sinan S.& Ozensoy O. (2004). "Purification of mulberry (Morus alba L.) polyphenol oxidase by affinity chromatography and investigation of its kinetic and electrophoretic properties." *Food Chemistry* **88**(3): 479-484.

[2] Chang L.H., J. T. T., Huang H.S., Nien Y.F., Chang C.M. J. (2006). "Supercritical carbon dioxide extraction of turmeric oil from Curcuma longa Linn and purification of turmerones." *Separation and Purification Technology* **47**(3): 119-125.

[3] Eigner D., S. D. (1999). "Ferula asa-foetida and Curcuma longa in traditional medical treatment and diet in Nepal." *Journal of Ethnopharmacology* **67**(1): 1-6.

[4] Fidler Isaiah J. (1975). "Biological behavior of malignant melanoma cells correlated to their survival in vivo." *Cancer Res* **35**(1): 218-224.

[5] Gabriela N., Raymond A. D.& Stefana M. P. (2005) "Tyrosinase-related protein-2 and -1 are trafficked on distinct routes in B16 melanoma cells." *Biochemical and Biophysical Research Communications* **328**(4): 914-921.

[6] Hye J. K., H. S. Y., Jin C. K., Chan S. P., Mi S. C., Mijee K., Hyangsoon C., Jung S. M., Yong S. K., Seong W. Y.& Jeong K. A. (2009). "Antiviral effect of Curcuma longa Linn extract against hepatitis B virus replication." *Journal of Ethnopharmacology* **124**(2,15): 189-196.

[7] Hsu, C.-K., Chang, C.-T., Lu, H.-Y. & Chung Y.-C. (2007) " Inhibitory effects of the water extracts of Lavendula sp. on mushroom tyrosinase activity ". *Food Chemistry* **105**(3), 1099-1105.

[8] Matsuda H., Nakashima S., Oda Y., Nakamura S.& Yoshikawa M.

(2009) "Melanogenesis Inhibitors from the rhizomes of *Alpinia officinarum* in B16 melanoma Cells." *Bioorganic & Medicinal Chemistry* **17**(16): 6048-6053.

[9] Madani W., Kermasha S.& Bisakowski B. (1999). "Inhibition of tyrosinase activity by a polyphenol esterase using selected phenolic substrates." *Phytochemistry* **52**(6): 1001-1008.

[10] Ng L.T., K. H.-H.& Lu T.M. (2009). "Potential antioxidants and tyrosinase inhibitors from synthetic polyphenolic deoxybenzoins." *Bioorganic & Medicinal Chemistry* **17**(13): 4360-4366.

[11] Ohguchi K., Banno Y., Akao Y. & Nozawa Y. (2004) "Involvement of Phospholipase D1 in Melanogenesis of Mouse B16 Melanoma Cells." *Biolobucal Chemistry* **279**(30): 3408–3412.

[12] Lee M. H., Lin Y. P., Hsu F. L., Zhan G. R.& Yen K. Y. (2006) "Bioactive constituents of *Spatholobus suberectus* in regulating tyrosinase-related proteins and mRNA in HEMn cells." *Phytochemistry* **67**(12): 1262–1270.

[13] Jiang Z., Xu J., Long M., Tu Z., Yang G.& He G. (2009) "2, 3, 5, 4′-tetrahydroxystilbene-2-O-β-d-glucoside (THSG) induces melanogenesis in B16 cells by MAP kinase activation and tyrosinase upregulation." *Life Sciences* **85**(9-10): 345-350.

嘉南藥理科技大學專題研究計畫成果報告

計畫編號：CN9802

計畫名稱：多酚化合物活性及有效成分探討— 子計畫二：川陳皮素(nobiletin)及其代謝產物 3',4'-dihydroxy-5,6,7,8-tetramethoxyflavone 對 LDL 氧化及脂泡細胞形成之影響

執行期間：98 年 1 月 1 日至 98 年 12 月 31 日

■整合型計畫　　□個別型計畫

計畫總主持人：楊朝成　　計畫主持人：

子計畫主持人：

一、楊朝成

二、吳明娟

三、葉東柏

中華民國 99 年 02 月 28 日

子計畫二：川陳皮素(nobiletin)及其代謝產物 3',4'-dihydroxy-5,6,7,8-tetramethoxyflavone 對 LDL 氧化及脂泡細胞形成之影響

子計畫二主持人: 吳明娟

ABSTRACT

There is accumulating evidence that LDL oxidation is essential for atherogenesis, and antioxidants that prevent oxidation may either decelerate or reduce atherogenesis. Current study focused on the effect and mechanism of 3',4'-dihydroxy-5,6,7,8-tetramethoxyflavone (DTF), a major metabolite of nobiletin (NOB, a citrus polymethoxylated flavone) on atherogenesis. We found DTF had stronger inhibitory activity than α-tocopherol on inhibiting Cu^{2+}-mediated LDL oxidation measured by thiobarbituric acid-reactive substances assay (TBARS), conjugated diene formation and electrophoretic mobility. Monocyte-to-macrophage differentiation plays a vital role in early atherogenesis. DTF (10-20 μM) dose-dependently attenuated differentiation along with the reduced gene expression of scavenger receptors, CD36 and SR-A, in both PMA- and oxidized low density lipoprotein (oxLDL)-stimulated THP-1 monocytes. Furthermore, DTF treatment of monocytes and macrophages lead to reduction of fluorescent DiI-acLDL and DiI-oxLDL uptake. In conclusion, at least three mechanisms are at work in parallel: DTF reduces LDL oxidation, attenuates monocyte differentiation into macrophage, and blunts uptake of modified LDL by macrophage. The effect is different from that of NOB, from which DTF is derived. This study thus significantly enhanced our understanding on how DTF may be beneficial against atherogenesis.

Keywords: low-density lipoprotein (LDL); atherogenesis; scavenger receptor A (SR-A); CD36

INTRODUCTION

Atherosclerosis is an inflammatory disease characterized by monocyte recruitment and cytoplasmic lipid accumulation within cells, leading to lipid-laden foam cells beneath the aortic endothelium [1]. Under oxidative stress, both blood monocytes and plasma lipoproteins invade the arterial wall, where they are exposed to atherogenic modifications [2]. In intima, monocytes were subsequently converted to macrophages, which express high level of scavenger receptors that bind modified LDL [3]. These processes give rise to the arterial foam cell, a hallmark of the arterial lesion [1]. Among the scavenger receptors, CD36, SR-A, and lectin-like oxidized LDL receptor-1 (LOX-1) represent the principal receptors in the process of foam cell formation [4, 5].

CD36, an 88-kDa membrane glycoprotein, plays a quantitatively significant role in modified LDL binding to macrophages [6]. In addition to binding acetylated LDL (acLDL) and oxidatively modified LDL (oxLDL), CD36 binds thrombospondin, anionic phospholipids, long-chain fatty acids and collagen [7]. CD36 is highly expressed on lipid-laden macrophages in human atherosclerotic aorta [8], possibly as a result of a positive feedback loop mediated by oxLDL and its lipid content [9, 10]. SR-A is a trimer of 77 kDa that binds to a diverse array of macromolecules including modified lipoproteins (acLDL or oxLDL), bacterial surface lipids (endotoxin and lipoteichoic acid), proteins modified by advanced glycation (advanced glycation end products, AGE), and β-amyloid fibrils [11]. LOX-1, a 50-kDa type II membrane glycoprotein, is expressed at very low levels in healthy endothelium but is upregulated by oxLDL or proinflammatory cytokines [12]. LOX-1 is also highly expressed by macrophages and smooth muscle cells in the intima of human carotid atherosclerotic plaques [13]. The natural ligand of LOX-1 is oxLDL, but not acLDL

[14]. The direct evidences of the involvement of scavenger receptors in atherosclerosis have been demonstrated using knockout mice [15-20] and these findings suggest that CD36, SR-A and LOX-1 play pro-atherogenic roles *in vivo*.

The oxidative hypothesis of atherosclerosis development has attracted extensive investigation of a possible preventive role of antioxidants [21, 22]. Dietary antioxidants, such as α-tocopherol or polyphenolics, not only protect LDL from oxidation but also reduce the development of atherosclerotic lesions [23-26]. Lots of studies have described their anti-atherogenic effects attributed to down-regulation of scavenger receptor gene expression in addition to antioxidant activities [26-30].

Strong *in vivo* [31, 32] evidence now exists to indicate that citrus flavonoids could reduce the occurrence of cardiovascular disease. *In vitro* data have demonstrated that these citrus flavonoids could reduce hepatic production of cholesterol containing lipoproteins [33] and induce hepatic LDL receptor gene transcription [34], and hence decrease total plasma cholesterol concentrations. In addition to the noted cholesterol lowering potential, it was reported that nobiletin (NOB, 5,6,7,8,3',4'-hexamethoxyflavone, **Figure 1**), a citrus polymethoxylated flavone, also attenuated scavenger receptor expression in PMA-induced THP-1 cells [35] and inhibited SR-A-mediated metabolism of acLDL in J774A.1 macrophages [36]. The di-demethylated metabolite of NOB, 3',4'-dihydroxy-5,6,7,8-tetramethoxyflavone (DTF, 3',4'-didemethylnobiletin; **Figure 1**), was found to exhibit stronger anti-inflammatory [37, 38] and anti-monocyte differentiation effects than its parent compound [39].

In this research, we aim to better understand the possible antiatherogenic effects and mechanisms of DTF in several aspects: (1) Cu^{2+}-induced LDL oxidation; (2) monocyte-to-macrophage differentiation; and (3) foam cell formation. The extent of

Cu^{2+}-induced LDL oxidation was studied by measuring the formation of conjugated dienes [40], and various aldehydic products (thiobarbituric acid-reactive substances, TBARS) [41] as well as changes of the electrophoretic mobility of apoB100 [42]. Monocyte-to-macrophage differentiation was investigated using THP-1 monocytes treated with PMA (30 nM) alone or PMA (1.6 nM) in combination with oxLDL (25 μg/ml). Foam cell formation was assessed by measuring the expression of scavenger receptors and modified LDL uptake in THP-1-derived macrophages. Our results clearly demonstrate that the anti-atherogenic effect of DTF is different from that of NOB, from which DTF is derived. There are at least three mechanisms at work in parallel for the effect: DTF reduces LDL oxidation, attenuates monocyte differentiation into macrophage, and blunts uptake of modified LDL by macrophages.

MATERIALS AND METHODS

Materials. Nobiletin (NOB) and 3',4'-dihydroxy-5,6,7,8-tetramethoxyflavone (DTF, 3',4'-didemethylnobiletin) were purified and synthesized as described before [38]. The RPMI 1640 medium, PMA (phorbol 12-myristate 13-acetate) and other chemicals were purchased from Sigma-Aldrich Co. (St. Louis, MO, USA) unless otherwise stated. Fetal bovine serum was from Hyclone (Logan, UT, USA). 1,1'-dioctadecyl-3,3,3',3'-tetramethylindocarbocyanide perchlorate (DiI) was from Invitrogen Life Technologies (Carlsbad, CA, USA).

Preparation and oxidation of LDL. LDL (d 1.019–1.063) was prepared from the plasma of healthy donors by sequential ultracentrifugation [43]. Lipoprotein was desalted and concentrated by ultra-filtration (Centricon 4, Amicon, Beverly, MA) against PBS at 450 × g, 4°C for 120 min. The protein concentration was measured by the method of Bradford [44], using bovine serum albumin as a standard.

OxLDL was prepared by incubation of LDL (0.2 mg of LDL protein/ml) with 10

μM Cu^{2+} in PBS at 37°C for 24 h followed by addition of 0.24 mM EDTA. The degree of LDL oxidation was determined by measurement of TBARS formation as described below. Lipoproteins for cell culture were sterilized by filtration through a 0.45 μm pore size filter (Gelman Sciences, Ann Arbor, MI) and stored at 4^{o}C.

Biochemical markers of lipid peroxidation.

Conjugated diene formation: Oxidation of LDL is accompanied by an increase in absorbance at 234 nm, due to the formation of conjugated dienes in constituent polyenoic fatty acids [45]. The quantity of conjugated dienes in LDL was assessed by monitoring the change at A234 at indicated time point [40].

Thiobarbituric acid-reactive substances (TBARS) formation: The formation of TBARS was determined based on the reaction of one molecule of malondialdehyde (MDA) with two molecules of thiobarbituric acid (TBA) to form a TBA-MDA adduct. The TBARS concentration was measured at 532 nm and expressed as MDA equivalents [46].

Electrophoresis of LDL: The electrophoresis mobility of LDL was used as an indication of protein oxidation and was measured using agarose gel. The Cu^{2+} mediated oxLDL was concentrated by ultra-filtration (Microcon YM-3, Amicon). About 1-2 μL of each concentrated sample was loaded onto Titan Lipoprotein Gel (Helena Laboratories, Beaumont, TX, USA) and run at 80 V for 45 min. Gel was then dried and stained with Fat Red 7B according to the manufacturer's instructions. Relative electrophoretic mobility (REM) was calculated as the mobility of oxLDL relative to that of native LDL (nLDL).

Cell culture. The monocyte-like cell line THP-1 was obtained from Bioresource Collection and Research Center (Hsinchu, Taiwan). THP-1 cells were cultured in RPMI 1640 medium, which contained 0.3 g/L L-glutamine, 4.5 g/L glucose, 10 mM

HEPES, 1.0 mM sodium pyruvate and 10% fetal bovine serum. Cell cultures were maintained at 37°C in a humidified 5% CO_2/95% air incubator.

For monocytic-to-macrophage differentiation, THP-1 monocytes were cultured in 6-well plates (1×10^6 cells/well) in RPMI-1640 medium supplemented with 30 nM of PMA, which is known to induce the maturation of monocytes, or with 1.6 nM of PMA together with 25 μg of oxLDL [47], as specified in each experiment for 24 h.

To prepare THP-1-derived macrophages, THP-1 monocytes were cultured in 6-well plates (1×10^6 cells/well) supplemented with PMA (200 nM) for 72 h. Non-adherent cells were then removed by washing the wells twice with RPMI.

mRNA expression of CD11b, SR-A, CD36 and LOX-1. Total cellular RNA was prepared using Illustra RNAspin Mini RNA Isolation Kit (GE Healthcare, Buckinghamshire, UK). Reverse-transcription was carried out using 1 μg RNA and High-Capacity cDNA Archive kit (Applied Biosystems, Foster City, CA, USA). Quantitative PCR was performed with 2 μL cDNA obtained above in 25 μL containing 200 nM primers using iTaq™ SYBR Green Supermix with ROX (BioRad, Hercules, CA, USA). The primer sequences for GAPDH, CD11b and scavenger receptors were deduced from PrimerBank [48] and listed in **Table 1**. Amplification was conducted in an ABI Prism 7300 sequence detection system. PCR conditions were as follows: 95 °C for 2 min, 40 cycles at 95 °C for 15 s, and 60 °C for 45 s. The optimal concentrations of primers and templates used were established based on the standard curve created before the reaction and corresponded to approximately 100% reaction efficiency. PCR results were then normalized to the expression of GAPDH in the same samples.

CD36 and SR-A phenotypic expression. Phenotypic expression of CD36 and SR-A were quantified by flow cytometry (FACScan, BD Biosciences, San Jose, CA,

USA). For detection of CD36 expression, cells (1×10^6) were resuspended in 100 μL PBS. Twenty μl fluorescein (FITC)-conjugated murine anti-human CD36 (clone FA6.152, Immunotech, Beckman Coulter, Fullerton, CA, USA) was added and incubated on ice for 60 min before washing twice with PBS. For detection of SR-A expression, cells (5×10^5) were resuspended in 100 μL PBS. Ten μL mouse anti-human SR-A/MSR1 antibody (25 μg/mL, clone 351615, R&D Systems, Minneapolis, MN, USA) was added and incubated at room temperature for 60 min. Cells were washed twice with PBS and then resuspended in 200 μL PBS. Ten μl FITC-labelled goat anti-mouse IgG antibodies (10 μg/mL, R&D Systems) were then added and incubated on ice for 60 min before washing twice with PBS. These cells were investigated in duplicates by flow cytometry (FACScan, BD Biosciences, San Jose, CA, USA). Data were acquired from 10,000 cells (events), and the fluorescent intensity was determined and expressed as the geometric mean fluorescence intensity (MFI).

Preparation of DiI-oxLDL and DiI-acLDL. LDL was incubated overnight at 37^{o}C under nitrogen and light protection with 50 μL of DiI (3 mg/ml in DMSO) for each milligram of LDL protein. The LDL must be labeled before acetylation or oxidation [49]. For preparation of DiI-oxLDL, DiI-LDL (0.1 mg/ml) was incubated with 10 μM Cu^{2+} in PBS at 37^{o}C in dark for 18 h [30]. Unbound dye and copper ions from the oxidation step described above which would otherwise be toxic to the cells were removed by passing through Sephadex G-25 (GE Healthcare). For preparation of DiI-acLDL, the method of Basu et al. [50] was employed. Unbound dye and acetate from acetylation step were then removed by passing through Sephadex-G25. Protein concentration of elute was determined by Bradford [44]. All lipoprotein preparations were stored at 4°C in sterile containers after filtration sterilization (0.45 μm).

Modified LDL uptake measurement by flow cytometry and fluorescent

microscopy. DiI-oxLDL or DiI-acLDL (10 μg/ml) was added into THP-1 monocytes or THP-1-derived macrophages and incubated for 24 h. The cells were washed with PBS and then examined with a fluorescence inverted microscope (IX-71, Olympus) followed by flow cytometry analysis (FACScan) using the FL2 emission filter. Data were acquired from 15,000 cells (events), and the DiI-oxLDL or DiI-acLDL uptake was determined and expressed as the geometric mean fluorescence intensity (MFI).

Statistical analyses. Student's *t*-tests were used to assess significant differences in parameters measured between in the presence and absence of test substances. The level of significance was set at $p<0.05$. All experiments have been performed at least three times.

RESULTS

Inhibition of LDL oxidation by DTF. It is recognized that oxidative modified low density lipoproteins (oxLDL) play an important role in the generation and progression of the atherosclerotic plaque [51]. When LDL is oxidized by radical generating substances or by Cu^{2+} ions, three consecutive phases of the reaction, naming lag phase, propagation phase and the decomposition phase, can be observed in kinetic experiments by measuring compositional changes of LDL [52]. As shown in the **top panel of Figure 2A**, incubation of LDL (0.1 mg/mL) with Cu^{2+} (10 μM) resulted in a significant increase in conjugated diene formation, with maximum at 7 h oxidation without detectable lag phase. Loading LDL with DL-α-tocopherol (AT, 5 μM) increased the length of the lag phase to 1 h and therefore delayed onset of propagation. In comparison, loading LDL with DTF (5 μM) resulted in distinct kinetic conjugated diene formation which exhibited four successive oxidation phases: a longer lag phase (3 h), the first propagation phase, an inhibition phase with a conjugated diene formation rate slower than in the first propagation phase and the

second propagation phase [53]. However, LDL loaded with nobiletin (NOB) did not show significant difference from that of vehicle.

To better measure the antioxidant activity of DTF, LDL oxidation was performed with lower concentration of DTF (0.5 or 1 μM) or higher concentration of AT (10 or 20 μM) **(bottom panel of Figure 2A)**. The conjugated diene formation of LDL supplemented with 1 μM of DTF or 20 μM of AT exhibited five successive phases (lag phase, the first propagation phase, an inhibition phase, the second propagation phase and a decomposition phase).

Incubation of LDL (0.1 mg/mL) with Cu^{2+} (10 μM) at 37°C for 3 h caused TBARS formation to increase from 0.95 ± 0.05 to 43.53±1.67 nmol MDA equivalent/mg LDL (**Figure 2B**). DTF treatment produced a dose-dependent reduction in TBARS formation, and IC_{50} was calculated as 1.14 ± 0.03 μM from linear regression curve. In parallel to the conjugated diene data, the antioxidant potency of DTF was significantly higher than positive control, AT, which had IC_{50} of 10.84 ± 0.95 μM.

To further investigate the protection of DTF towards electronegative charge modification of LDL-protein moiety (apoB) induced by Cu^{2+}, agarose gel electrophoresis was carried out as described in Materials and Methods. Native LDL (nLDL, 0.1 mg/mL) treated with Cu^{2+} (10 μM) for 3 h increased REM to 3.03 (**Figure 2C)**. Oxidation of LDL in the presence of 5 μM DTF resulted in decreased REM to 1.13. On the other hand, LDL treated with 5 μM NOB or AT exhibited less protective effect against Cu^{2+}-mediated electronegative charge modification of apoB.

DTF inhibits monocyte-to-macrophage differentiation. The human monocytic cell line THP-1 was used as a model system to analyze gene expresssion and activity involved in monocyte-to-macrophage differentiation [54]. To evaluate the maximal

dosages of NOB and DTF could be used in THP-1 monocytes and macrophages, cell viability was analyzed using 3-(4,5-dimethylthiazol-2-yl)-2,5- diphenyltetrazolium (MTT) assay [55]. Our result demonstrates that 50 μM NOB and DTF exhibited significant (33~36%) cytotoxicity in THP-1 monocytes after 48 h incubation; while lower doses (10 and 20 μM) did not show significant adverse effect. A similar phenomenon was observed in THP-1 derived macrophages (data not shown). The differentiation-inducing dose of 30 nM PMA and working duration of 24 h was also determined in preliminary dose response experiments by analyzing differentiation marker CD11b expression and morphology change (data not shown).

THP-1 monocytes, which were originally in suspension, were treated with indicated concentrations of NOB or DTF 30 min prior to the addition of PMA (30 nM) for 24 h. The mRNA expression of differentiation marker, CD11b, and the major scavenger receptors, naming CD36, SR-A and LOX-1, measured by RT-Q-PCR normalized to the level of GADPH is shown in **Figure 3**. CD11b expression was increased by 17.0 ± 1.6 folds when THP-1 monocytes were treated with PMA (30 nM) for 24 h (**Figure 3A**). This is in a good agreement with the well-known theory that differentiation of monocytes into tissue macrophages results in an increase in mRNA and surface of CD11b/CD18 expression [56]. Addition of DTF (10 and 20 μM) in the process of monocyte differentiation dose-dependently inhibited CD11b mRNA expression, indicating the differentiation was attenuated. On the other hand, NOB had no influence on PMA-stimulated CD11b expression.

As expected, THP-1 monocytes exhibited very low level of LOX-1 mRNA and treated with PMA (30 nM) for 24 h induced more than 1000-fold increase (**Figure 3B**). Treatment of THP-1 cells with DTF or NOB strongly attenuated PMA-induced LOX-1 expression and the percentage of reduction was 81.4%, 98.8%, 58.9% and

79.4% for 10 μM DTF, 20 μM DTF, 10 μM NOB and 20 μM NOB, respectively, as compared with PMA-treated cells (p<0.01).

The impact of DTF and NOB on CD36 expression during PMA-stimulated monocyte differentiation is shown in **Figure 3C**. THP-1 monocytes exhibited little CD36 mRNA expression, while PMA-treated cells increased CD36 expression by 26.8 ± 0.4 folds. THP-1 monocytes treated with DTF significantly suppressed PMA-stimulated CD36 mRNA expression dose-dependently and 20 μM DTF can down-regulated CD36 mRNA to the level of monocytes. Surprisingly, NOB induced CD36 mRNA expression during THP-1 differentiation.

Figure 3D further demonstrates the effects of NOB and DTF on SR-A transcript expression in THP-1 monocytes treated with PMA (30 nM) for 24 h. It was found that PMA induced about 480-fold SR-A mRNA expression and addition of 10 μM and 20 μM DTF reduced PMA-induced SR-A expression by 56.8% and 98.6%, respectively. However, no effect was observed for NOB-treated cells.

CD36 and SR-A are the principal receptors responsible for the binding and uptake of modified LDL in macrophages and together these two receptors account for 75 to 90% of the uptake and degradation of acetylated and oxidized LDL [57]. We thus further studied the effects of NOB and DTF on CD36 and SR-A surface protein level using flow cytometry as described in Materials and Methods. Data demonstrated that the expression of CD36 and SR-A surface protein increased by 6.3- and 1.9-fold, respectively (**Figures 3E and F**). Addition of 20 μM DTF could significantly reduced surface CD36 and SR-A protein expression by 80.5% and 41.8% (p<0.01 and 0.05), respectively, as compared with PMA-treated cells. On the other hand, treatment of THP-1 cells with NOB or lower dose of DTF did not have significant effect on CD36 or SR-A surface protein expression.

The LDL particle acquires a number of important biological activities as a result of oxidative modification in addition to the ability to bind scavenger receptors. OxLDL is both a potent chemoattractant for circulating monocytes and a potent inhibitor of resident macrophage motility [58]. Previous studies have indicated that oxLDL plays a role in promoting differentiation of monocytes to macrophages [59, 60]. Recently, it has been reported that treatment of THP-1 monocytes with oxLDL plus 1.6 nM of PMA resulted in a dramatic synergistic effect on differentiation as compared with oxLDL alone [47]. By RT-Q-PCR analysis, we also observed that in the presence of 1.6 nM of PMA, CD36 mRNA expression of THP-1 monocytes increased with oxLDL concentration (5-25 μg/ml) (data not shown). mRNA transcripts for CD36, SR-A and LOX-1 were increased following cell treatment with oxLDL (25 μg/ml) by up to 1.5-, 1.7- and 2.2-fold, respectively, after 24 h culture as compared with PMA (1.6 nM) alone (**Figure 4**). DTF (20 μM) could significantly reduce the transcripts of CD36, SR-A and LOX-1 (p<0.01, 0.05 and 0.05, respectively). On the contrary, NOB did not exert any detectable inhibitory effect on any of the gene expression (data not shown).

It has been well-known that differentiated monocytes exhibit characteristic macrophage activity, i.e., increased cellular uptake of oxLDL**.** Our next approach was to examine whether NOB and DTF could block modified LDL uptake associated with monocyte differentiation. THP-1 monocytes were pre-treated with vehicle or indicated concentration of NOB or DTF for 30 min prior to exposure to PMA (30 nM) for 24 h. These cells were then incubated with DiI-acLDL (10 μg/mL) for 24 h. Accumulation of DiI-acLDL into the cytoplasm was observed by fluorescence microscopy (vehicle of **Figure 5A**). Addition of DTF or NOB (10 and 20 μM) dose-dependently abolished acLDL uptake. In parallel, flow cytometry (**Figure 5B)**

shows that 10 and 20 μM DTF inhibited PMA-induced DiI-acLDL uptake by 61.5 and 86.2%, respectively. Lower concentration of NOB (10 μM) did not affect PMA-induced DiI-acLDL uptake, while higher concentration (20 μM) inhibited only 30.0% uptake.

Fluorescence microscopy **(Figure 5C)** also demonstrates that treatment of THP-1 monocytes with PMA (30 nM) for 24 h stimulated DiI-oxLDL uptake dramatically. In parallel, flow cytometry (**Figure 5D)** revealed PMA increased 25-fold DiI-oxLDL uptake as compared with monocytes. Treatment of THP-1 monocytes with DTF and NOB (10-20 μM) dose-dependently inhibited PMA-stimulated DiI-oxLDL uptake by 68.8-88.4% and 26.2-67.3%, respectively.

DTF inhibits the expression and activity of scavenger receptors in THP-1-derived macrophages. THP-1-derived macrophages have been extensively used as a model for studies of scavenger receptor expression and foam cell formation in response to various agents [61-63]. THP-1 monocytes were first allowed to differentiate into adherent macrophages by PMA (200 nM) for 3 days prior to exposure to test agent for 48 h. It has been shown that SR-A and CD36 are responsible for the preponderance of modified LDL uptake in macrophages and that other scavenger receptors do not compensate for their absence [57]. As a consequence, we investigated whether DTF or NOB treatment could inhibit foam cell formation by focusing on SR-A and CD36 expression and modified LDL uptake. **Figure 6** shows that the mRNA expression of CD36 and SR-A of THP-1-derived macrophages was significantly repressed by DTF in a dose-dependent manner. About 46.1 ± 3.4 and 12.6 ± 2.8% of CD36 expression was detected in 10 and 20 μM DTF-treated THP-1 macrophages, respectively, relative to vehicle (**Figure 6A**). NOB (10-20 μM) was less potent and inhibited about 40% of CD36 expression with no clear dose response.

Likewise, SR-A expression in THP-1 macrophages was significantly inhibited by DTF (10-20 μM) by 68-92% dose-dependently. NOB inhibited SR-A expression by about 55% without dose-response relationship (**Figure 6B**).

DiI-oxLDL and DiI-acLDL uptake was studied to determine the effects of NOB and DTF on scavenger receptor activity. Fluorescence microcopy of **Figure 6C** shows that the uptake of DiI-oxLDL was highly enhanced in THP-1 macrophages and the addition of DTF or NOB significantly reduced the number of fluorescent cells. In parallel, flow cytometry of **Figure 6D** shows that treatment of THP-1 macrophages with DTF and NOB (10-20 μM) dose-dependently inhibited DiI-oxLDL fluorescence signal by 45-80 and 34-68%, respectively. Similar effect was observed for DiI-acLDL uptake into macrophages (**Figure 6E**).

DISCISSION

Oxidative modification of LDL is believed to be an important event in atherogenesis [64], and several studies have reported on the antioxidant effect of flavonoids, that is, decreasing the susceptibility of LDL to oxidation [65-68]. To study the effect of 3',4'-dihydroxy-5,6,7,8-tetramethoxyflavone (DTF), as antioxidants in preventing copper-induced oxidation of LDL, three different approaches were employed to measure changes in parameters known to be associated with LDL oxidation: formation of conjugated dienes and thiobarbituric acid reactive substances (TBARS) during lipid peroxidation, as well as increase in the electrophoretic mobility of LDL due to apolipoprotein B100 modification [69]. In agreement with previous study [53], we found that artificial enhancement of antioxidant defenses by increasing α-tocopherol (AT) concentration (from 5 to 20 μM) invariably made LDL more resistant to peroxidative modifications as extended lag phase shown in **Figure 2**. Both LDL loaded with AT (20 μM) or DTF (1 μM) showed five successive oxidation

phases: lag phase, the first propagation phase, an inhibition phase, the second propagation phase, and a decomposition phase. It has been suggested that the delayed onset of the second propagation (**Figure 2**) may reflect the chain-breaking activity of AT to halt the progression of lipid peroxidation and the second inhibition phase is a period where AT is being consumed via peroxyl radical scavenging [53]. Consequently**,** a rise in the second inhibition phase for LDL enriched with AT (shown in **bottom panel of Figure 2A**) may be due to lipid hydroperoxides (LOOH) formation via the reaction with AT. Although no termination phase was observed for LDL enriched with DTF (5 μM) in **top panel of Figure 2A**, the oxidation would have stop if we had extended incubation longer. In addition to chain breaking activity, DFT might have a metal binding activity which would reduce the overall rate of initiating radical generation.

A key feature of LDL oxidation is the breakdown of polyunsaturated fatty acids to yield a broad array of smaller fragments, 3–9 carbons in length, including aldehydes and ketones [70]. As a result, besides evaluating the conjugated dienes that form following the Cu^{2+}-triggered peroxidation, we also studied the accumulation of TBARS for LDL supplemented with DTF or AT after 3 h oxidation (**Figure 2B**). The data presented and obtained by utilizing these two different analytical procedures, clearly demonstrate that DTF has about 10- to 20-fold higher antioxidant activity as compared with AT; while NOB has negligible antioxidant activity.

It has been found that malondialdehyde (or other aldehydes) generated during oxidation can form Schiff bases with the ε-amino groups of lysine residues of apoB [71]. In this research, we also found that the relative electrophoretic mobility (REM) of LDL increased in the presence of Cu^{2+} and the addition of DTF (5 μM) could significantly protect apoB from oxidative modification. NOB had no detectable

antioxidant effect; while AT (5 μM) had limited inhibitory activity against conjugated diene formation (**Figure 2A**) and TBARS formation **(Figure 2B)**. As a result, these characteristics might explain why there was no significant difference in REM assay between LDL enriched with AT or NOB and vehicle control (**Figure 2C)**.

In atherosclerotic lesions, monocytes migrate into the vessel wall and differentiate into macrophages. Some macrophages become lipid-loaded after uptake of oxLDL. As a result, to mimic events in atherosclerotic lesions, both monocyte-to-macrophage differentiation and foam cell formation need to be studied [72]. In this study, we first used PMA- and oxLDL-stimulated THP-1 cells as models to study the effects of NOB and DTF on monocyte differentiation. The expression of scavenger receptors is upregulated during the differentiation of monocytes into macrophages, which is a key event in the process of atherosclerosis. It was found that THP-1 monocytes stimulated with PMA (30 nM) for 24 h significantly induced CD11b, LOX-1, CD36 and SR-A mRNA expression by ~17, >1000, ~27 and ~480 folds, respectively (**Figures 3A-D**). These levels were higher than those published by using semi-quantitative RT-PCR in combination with end-product gel electrophoretic analysis [35, 39, 47]. Phenotypic expression analyzed by flow cytometry further demonstrated that PMA (30 nM) induced CD36 and SR-A surface protein expression by 6.3- and 1.9-fold (**Figures 3E and F**). The protein induction was similar to those published in literature [47] but was much lower than that of mRNA. The discrepancy between induction of mRNA and surface protein expression might be caused by (1) the newly made mRNA does not completely contribute to the protein synthesis or the turnover rate of mRNA is relatively slow so that detected mRNA level is higher; (2) nascent protein does not completely translocate from the intracellular compartments to cellular surface so that surface protein level is lower [73]; (3) RT-Q-PCR has higher

detection sensitivity than flow cytometry.

Current result (**Figure 3**) also showed that DTF (10 and 20 μM) could attenuate monocyte-to-macrophage differentiation because the transcripts of CD11b, LOX-1, CD36 and SR-A, as well as surface CD36 and SR-A protein expression were significantly reduced in a dose-dependent manner. On the other hand, the effect of parent compound, NOB, on monocyte differentiation was distinct. In the mRNA expression, NOB had no effect on CD11b or SR-A; while decreased LOX-1 and increased CD36. These results are slightly different from those published by Eguchi et al. [35, 39], which demonstrated that both NOB and DTF could reduce LOX-1, SR-A, and CD36 mRNA levels. We reasoned that these discrepancies may be accounted by variations in THP-1 culture condition and primer design for the target gene or detection limit difference between the real-time PCR and traditional PCR [74].

It has been well-known that oxLDL, in contrast to native LDL, induces a differentiation process in monocytes, resulting in a more mature macrophage-like phenotype [60]. Stimulation of monocyte-to-macrophage differentiation was dependent on the extent of LDL oxidation, and required oxLDL internalization by the cells [47]. Current research (**Figure 4**) demonstrated that DTF, rather than NOB, downregulated oxLDL-stimulated scavenger receptor expression. Among these scavenger receptors, the expression of CD36 was the most sensitive to DTF treatment. It has been indicated that there might be different pathways activated by oxLDL and PMA. PKB/PPARγ signaling pathways are thought to mediate CD36 expression in response to oxLDL [75]; while PKC/PPARγ is to mediate PMA-induced differentiation [75, 76]. From the current result, it is likely that DTF rather than its parent compound, NOB, interferes with both pathways.

The above results led us to examine whether DTF and NOB can affect

differentiation-associated scavenger receptor activity by measuring uptake of acLDL and oxLDL. AcLDL is known to be bound to and taken up mainly through SR-A; while a less extent is through CD36. OxLDL is taken up, for the most part, through CD36; while through SR-A and LOX-1 in a less degree. Fluorescence microscope (**Figures 5A and C**) provided live-cell imaging of increased number of fluorescence cells in response to PMA. Flow cytometry (**Figures 5B and D**) revealed 6-fold DiI-acLDL and 25-fold DiI-oxLDL mean fluroscence (MFI) increase in PMA-treated cells as compared with monocytes. The increase is associated with PMA-induced expression and activities of scavenger receptors. Treatment of THP-1 cells with DTF (10-20 μM) during differentiation dose-dependently block PMA-stimulated uptake of modified LDL by 61-88% (**Figure 5**). This effect may result from the combined decrease of SR-A, LOX-1 and CD36 expression (**Figure 3**). In comparison, NOB decreased PMA-stimulated DiI-acLDL and DiI-oxLDL uptake, in less extent (**Figure 5**); although it did not suppress PMA-induced SR-A or CD36 mRNA or surface protein expression (**Figure 3**). This result was similar to the effect of NOB in murine J774A.1 macrophages [36]. We also found that NOB exhibited stronger inhibitory effect against DiI-oxLDL uptake than DiI-acLDL uptake and this may be associated with its inhibition on LOX-1 mRNA expression. Nevertheless, the attenuation of modified LDL uptake by NOB could not be completely explained by merely down-regulation of scavenger receptor expression, it is likely that NOB function downstream of scavenger receptor ligand binding as well.

We further questioned whether DTF and NOB also inhibited foam cell formation in THP-1-derived macrophages. RT-Q-PCR (**Figures 6A and B**) indicated that addition of DTF and NOB markedly inhibited the expression of SR-A and CD36, which were responsible for the majority of modified LDL processing in macrophages

[57]. To elucidate whether there are any functional consequences for DTF- or NOB-mediated inhibition of SR-A and CD36 expression, quantitative analysis of DiI-acLDL and DiI-oxLDL uptake was performed in THP-1-derived macrophages. Both DTF and NOB significantly inhibited DiI-acLDL as well as DiI-oxLDL uptake by THP-1 macrophages dose-dependently. It appears that both DTF and NOB exert dual effects in inhibiting SR-A and CD36 activities in macrophages. By comparing data from **Figure 3** to **Figure 6**, it is apparent that the effect of NOB on scavenger expression and activity is more evident in macrophages than during monocyte-to-macrophage differentiation.

It has been generally accepted that catechol compounds which possess two adjacent OH-groups in the benzene ring can be further oxidized to reactive semiquinone, which may bring about the pharmacological or toxicological activities [77]. Similarly, DTF has been reported stronger anti-inflammatory and antitumor activity than NOB [37]. In this research we further demonstrated that DTF exerts a stronger protective effect against atherogenesis than NOB because of its stronger antioxidant activity against LDL oxidation and its potent inhibitory effect against monocyte-to-macrophage differentiation and foam cell formation. This observation, if confirmed *in vivo*, might have important clinical implications in the prevention and treatment of atherosclerosis.

ACKNOWLEDGEMENTS

Critical reviews and suggestions from Professor Verne N. Schumaker and Professor Chenbei Chang are very much appreciated. This research was supported by Grants NSC-96-2320-B-041-006-MY3 (to Dr. M-J Wu) and NSC-98-2313-B-041 -002-MY3 (to M.-C. Kou) from the National Science Council, Taiwan and Campus Integrated Project Grant (to Dr. M-J Wu) from Chia Nan University, Taiwan.

Table 1. Primer pairs used in RT-Q-PCR.

Gene	Sequence (5'-3')	Amplicon (bp)
GAPDH	CATGAGAAGTATGACAACAGCCT AGTCCTTCCACGATACCAAAGT	113
CD36	GCCAAGGAAAATGTAACCCAGG GCCTCTGTTCCAACTGATAGTGA	101
SR-A	GCAGTGGGATCACTTTCACAA AGCTGTCATTGAGCGAGCATC	85
LOX-1	CTCGGGCTCATTTAACTGGGA AGGAAATTGCTTGCTGGATGAA	113
CD11b	ACTTGCAGTGAGAACACGTATG AGAGCCATCAATCAAGAAGGC	141

Figure 1. Chemical structures of nobiletin and 3',4'-dihydroxy-5,6,7,8-tetramethoxyflavone.

Figure 2. Effects of 3',4'-dihydroxy-5,6,7,8-tetramethoxyflavone (DTF), nobiletin (NOB), and DL-α-tocopherol (AT) on inhibiting Cu^{2+}-induced LDL oxidation. Native LDL (nLDL) (0.1 mg/ml) was oxidized with 10 μM Cu^{2+} in the presence of vehicle (0.1% DMSO) or indicated compound at 37°C. (**A**) The formation of conjugated diene was measured by change in absorbance at 234 nm (ΔA234) after oxidation for the indicated period. (**B**) TBARS formation was measured after oxidization for 3 h as described in Materials and Methods. (**C**) Electrophoretic mobility was measured in the presence of 5 μM of indicated compound as described in Materials and Methods.

Figure 3. Effects of 3',4'-dihydroxy-5,6,7,8-tetramethoxyflavone (DTF) and nobiletin (NOB) on the mRNA expression of CD11b (**A**), LOX-1 (**B**), CD36 (**C**) and SR-A (**D**); as well as surface protein expression of CD36 (**E**) and SR-A (**F**) during monocyte-to-macrophage differentiation. THP-1 monocytes were treated with vehicle (0.1% DMSO), DTF or NOB for 30 min prior to 30 nM PMA addition and incubated for 24 h. To measure mRNA expression, total cellular RNA was prepared and the expression of mRNA was analyzed as described in Materials and Methods. The data were normalized with reference to the expression levels of the corresponding GAPDH mRNAs. Data represent mean ratio± SEM of three independent experiments relative to the value of the monocytes (**A-D**). Cell surface CD36 protein expression was measured by incubation cells with fluorescein (FITC)-conjugated murine anti-human CD36 (clone FA6.152, Immunotech, Beckman Coulter). Cell surface SR-A expression was measured by incubation cells with mouse anti-human SR-A/MSR1 antibody

(clone 351615, R&D Systems) followed by FITC-labelled goat anti-mouse IgG antibodies. The level of fluorescence was investigated in duplicates by flow cytometry (Coulter EPICS XL, Beckman Coulter) as described in Materials and Methods (**E and F**). *, $p<0.05$ and **, $p < 0.01$ represents significant differences compared with vehicle control of 30 nM PMA-treated cells.

Figure 4. Effects of 3',4'-dihydroxy-5,6,7,8-tetramethoxyflavone (DTF) on the mRNA expression of CD36, SR-A and LOX-1 in oxLDL-induced monocyte-to-macrophage differentiation. THP-1 monocytes were treated with vehicle (0.1% DMSO), NOB for 30 min prior to 1.6 nM PMA and 25 μg/mL oxLDL treatment and incubated for 24 h. Total cellular RNA was prepared and the expression of mRNA was analyzed as described in Materials and Methods. The data were normalized with reference to the expression levels of the corresponding GAPDH mRNAs. Data represent the mean ratio ± SEM of three independent experiments relative to the value of the PMA (1.6 nM)-treated cells. *, $p<0.05$ and **, $p<0.01$ represent significant differences compared with cells treated with PMA (1.6 nM) plus oxLDL (25 μg/mL).

Figure 5. Effects of 3',4'-dihydroxy-5,6,7,8-tetramethoxyflavone (DTF) and nobiletin (NOB) on DiI-acLDL and DiI-oxLDL uptake in PMA-stimulated THP-1 monocytes. THP-1 monocytes were treated with vehicle (0.1% DMSO), DTF or NOB for 30 min prior to PMA (30 nM) addition and incubated for 24 h. DiI-acLDL (**A** and **B**) and DiI-oxLDL (**C and D**) (10 μg/mL) was added to cells and incubated for 24 h. Cell association of DiI-modified LDL was observed under fluorescence microscopy (**A** and **C**). Cells were then analyzed by flow cytometry (**B** and **D**) as described in

Material and Methods. Data represent the mean ± SEM of three independent experiments. *, $p<0.05$ and **, $p<0.01$ represent significant differences compared with vehicle control of 30 nM PMA-treated cells.

Figure 6. Effects of 3',4'-dihydroxy-5,6,7,8-tetramethoxyflavone (DTF) and nobiletin (NOB) on the mRNA expression of CD36 (**A**) and SR-A (**B**) and DiI-modified LDL uptake (**C-E**) in THP-1-derived macrophages. THP-1-derived macrophages were treated with vehicle (0.1% DMSO), DTF or NOB for 48 h. To measure mRNA expression level, total cellular RNA was prepared and analyzed as described in Materials and Methods. The data were normalized with reference to the expression levels of the corresponding GAPDH mRNAs and were represented as the mean ratio ± SEM of three independent experiments relative to the value of the vehicle-treated cells (**A and B**). To measure modified LDL uptake, DiI-oxLDL or DiI-acLDL (10 μg/ml) was added to cells and incubated for another 24 h. Cell association of DiI-oxLDL was observed under fluorescence microscopy (**C**) and the uptake of DiI-modified LDL was quantitated by flow cytometry (**D** and **E**). Data represent the mean ± SEM of three independent experiments.*, $p<0.05$ and **, $p < 0.01$ represent significant differences compared with vehicle control.

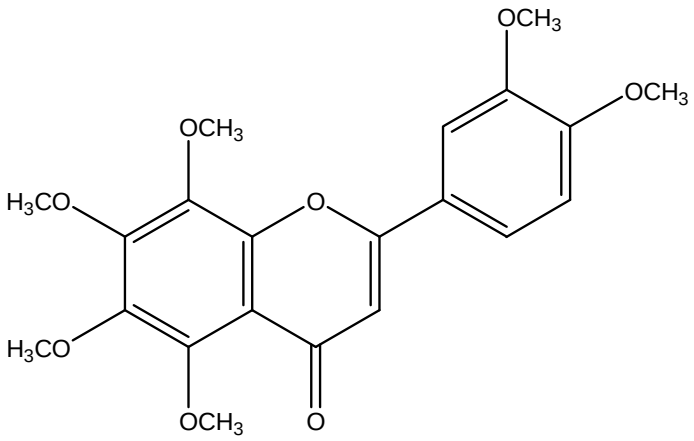

Nobiletin

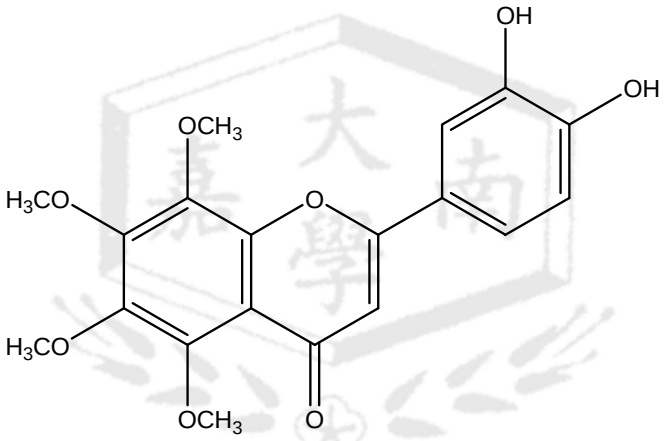

3',4'-dihydroxy-5,6,7,8-tetramethoxyflavone

(Figure 1)

A Conjugated Diene Formation

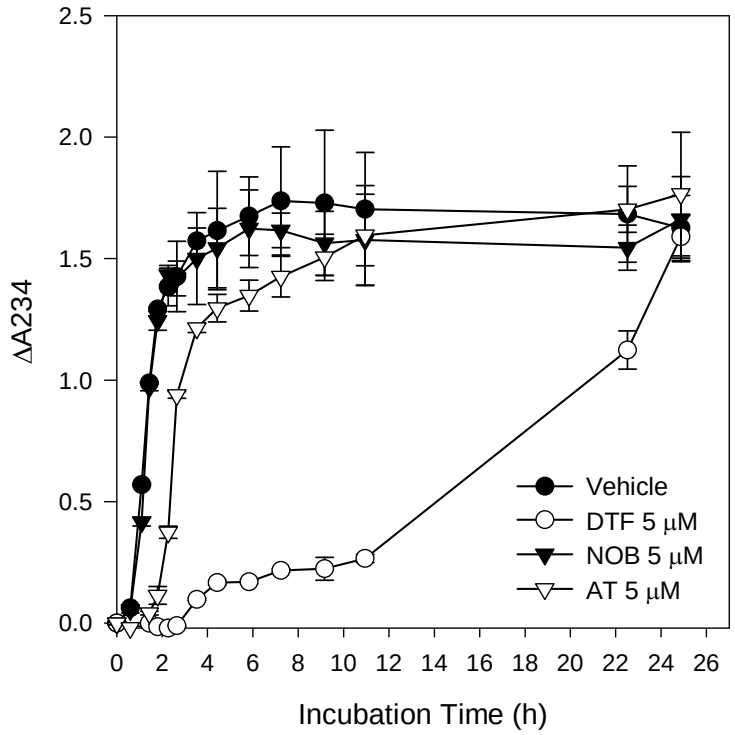

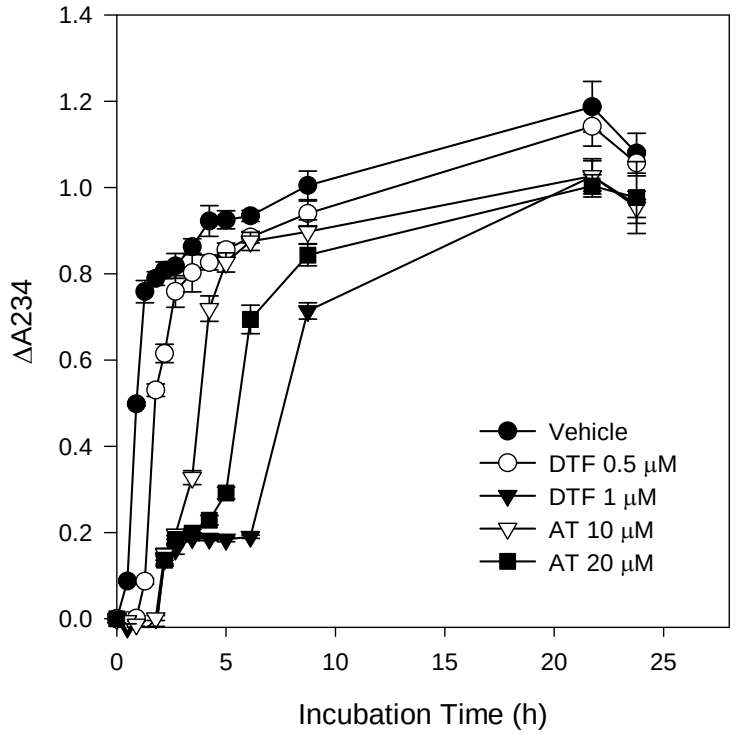

(Figure 2A)

B

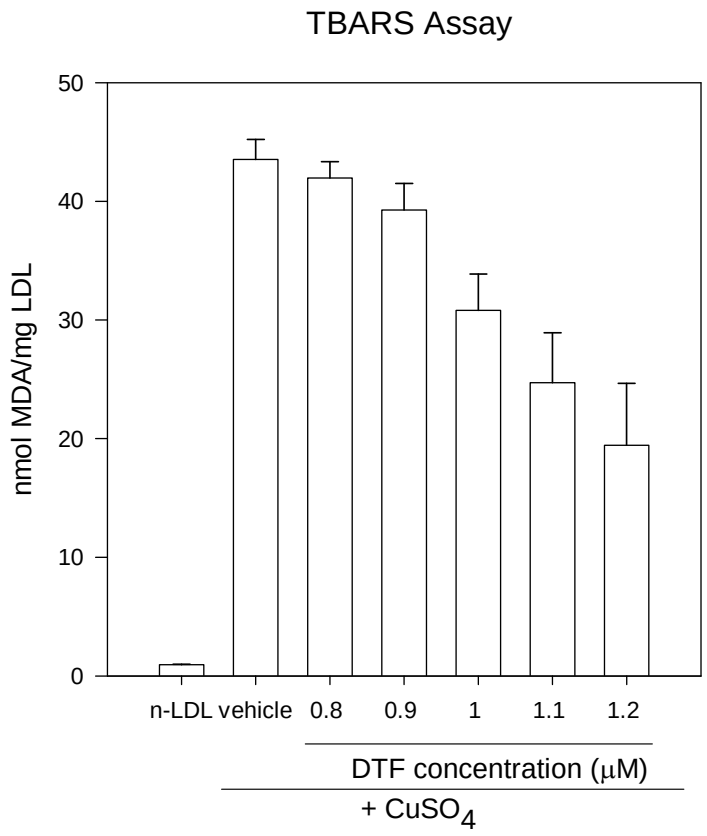
TBARS Assay
nmol MDA/mg LDL
50
40
30
20
10
0
n-LDL
vehicle
0.8
0.9
1
1.1
1.2
DTF concentration (μM)
+ CuSO4

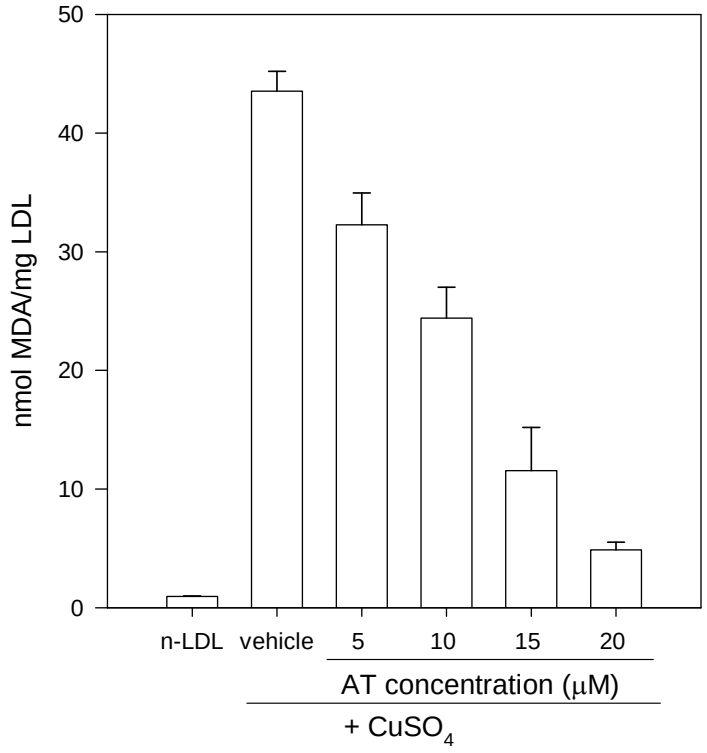
nmol MDA/mg LDL
50
40
30
20
10
0
n-LDL
vehicle
5
10
15
20
AT concentration (μM)
+ CuSO4

(Figure 2B)

C

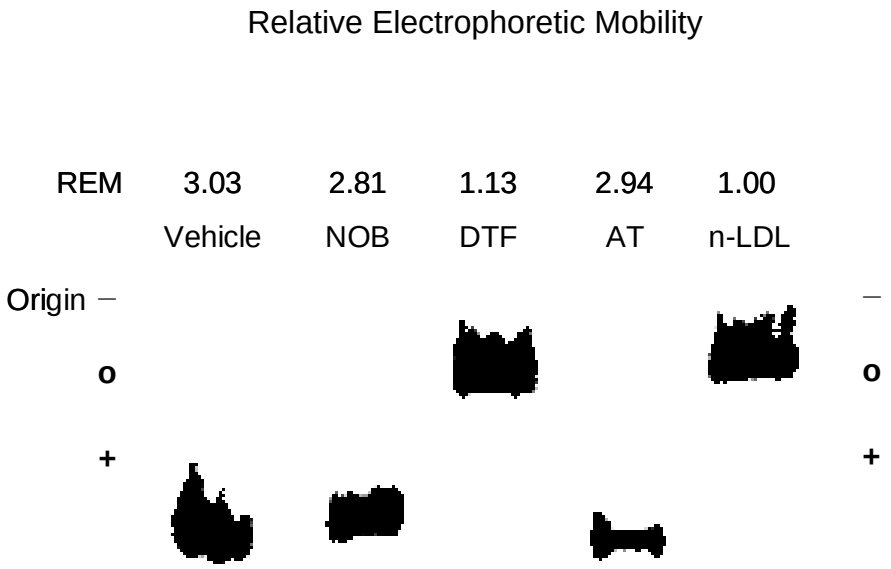
Relative Electrophoretic Mobility
REM
3.03
2.81
1.13
2.94
1.00
Vehicle
NOB
DTF
AT
n-LDL
Origin
o
+
−
o
+

(Figure 2C)

A

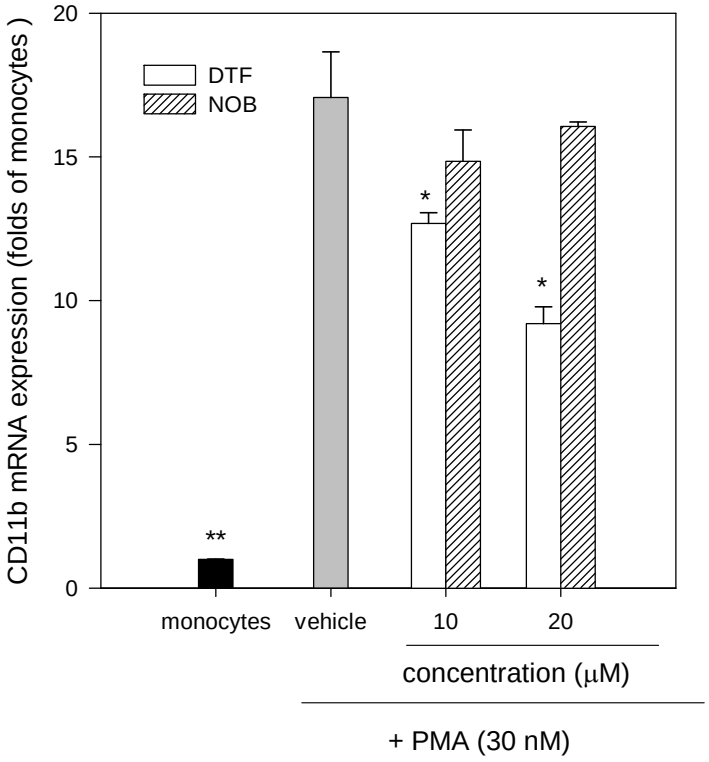

B

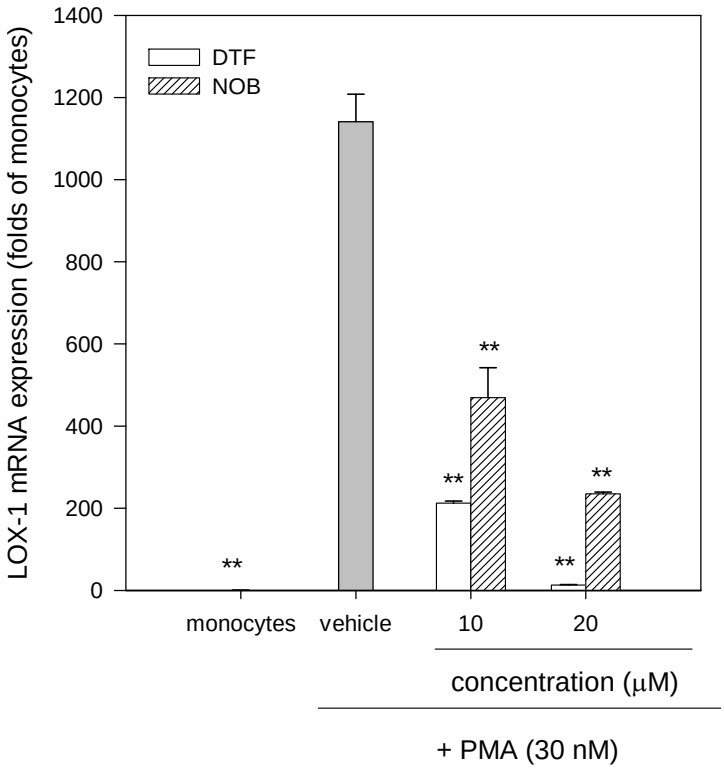

(Figure 3 A,B)

C

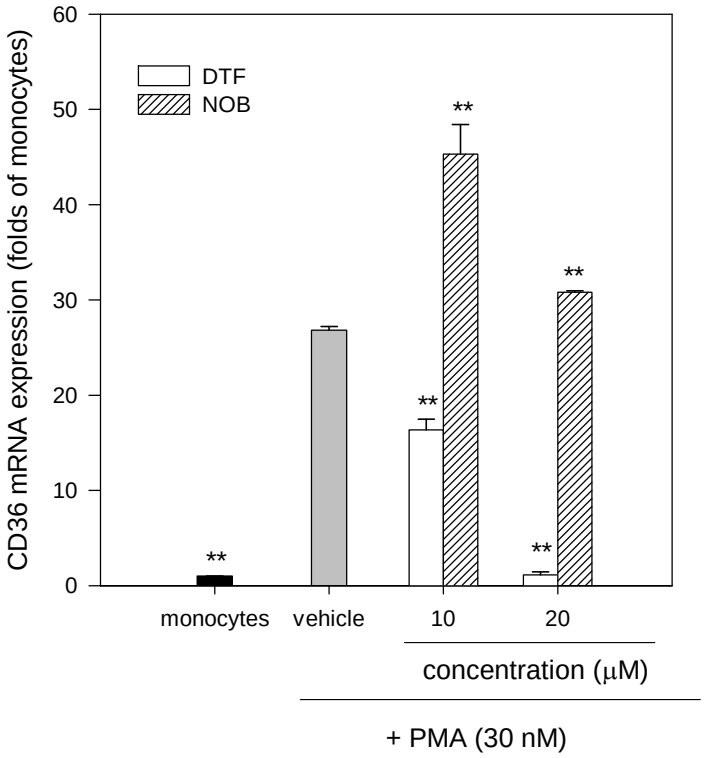

D

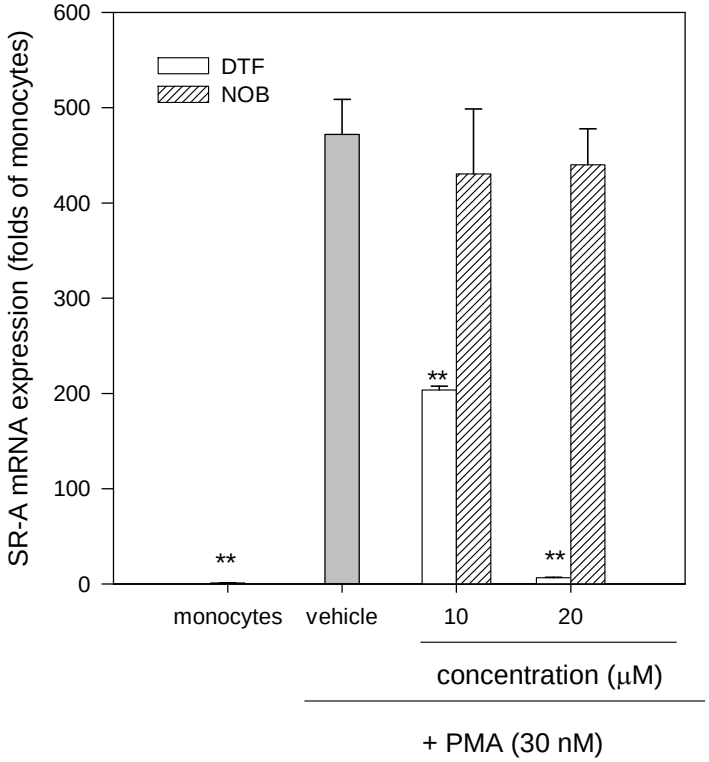

(Figure 3 C,D)

E

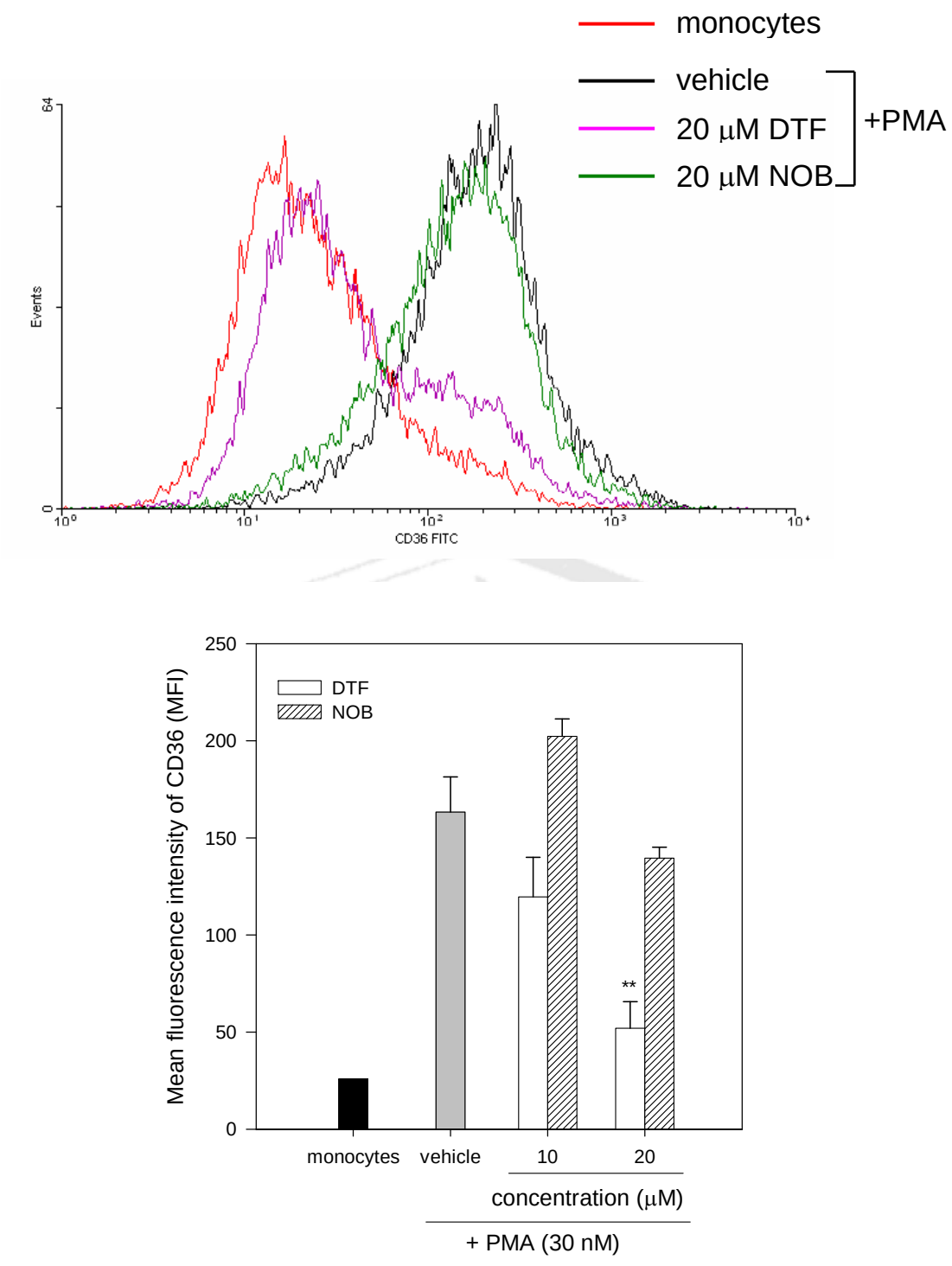
monocytes
vehicle
20 μM DTF
20 μM NOB
+PMA
64
Events
0
10^0
10^1
10^2
10^3
10^4
CD36 FITC
250
200
150
100
50
0
Mean fluorescence intensity of CD36 (MFI)
DTF
NOB
**
monocytes
vehicle
10
20
concentration (μM)
+ PMA (30 nM)

(Figure 3E)

F

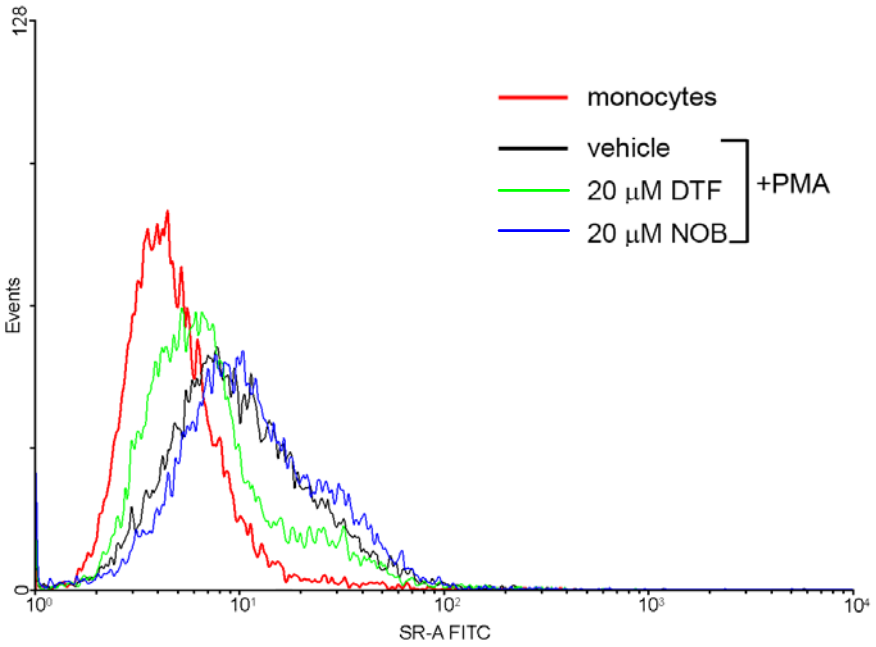
128
Events
0
monocytes
vehicle
20 μM DTF
20 μM NOB
+PMA
10⁰
10¹
10²
10³
10⁴
SR-A FITC

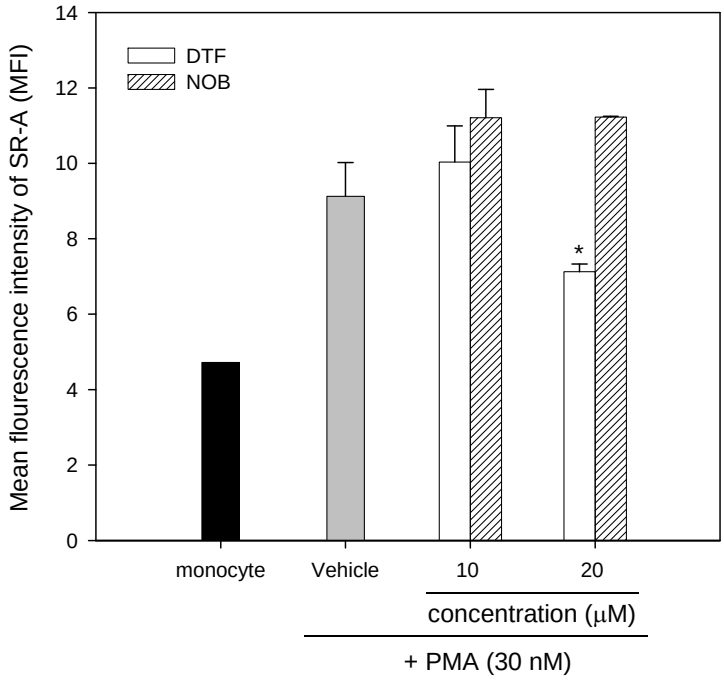
Mean flourescence intensity of SR-A (MFI)
DTF
NOB
14
12
10
8
6
4
2
0
*
monocyte
Vehicle
10
20
concentration (μM)
+ PMA (30 nM)

(Figure 3F)

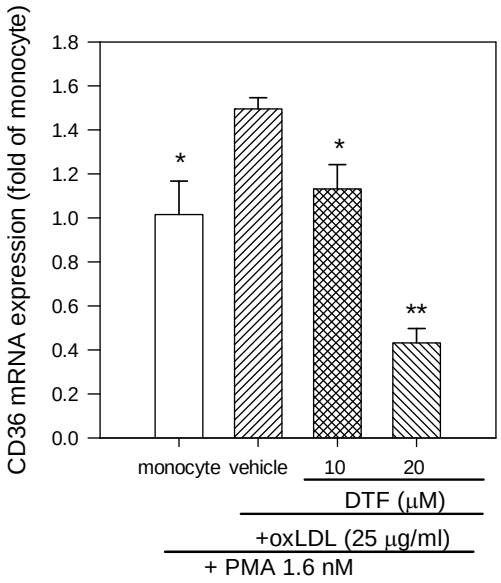
CD36 mRNA expression (fold of monocyte)
1.8
1.6
1.4
1.2
1.0
0.8
0.6
0.4
0.2
0.0
*
*
**
monocyte
vehicle
10
20
DTF (μM)
+oxLDL (25 μg/ml)
+ PMA 1.6 nM

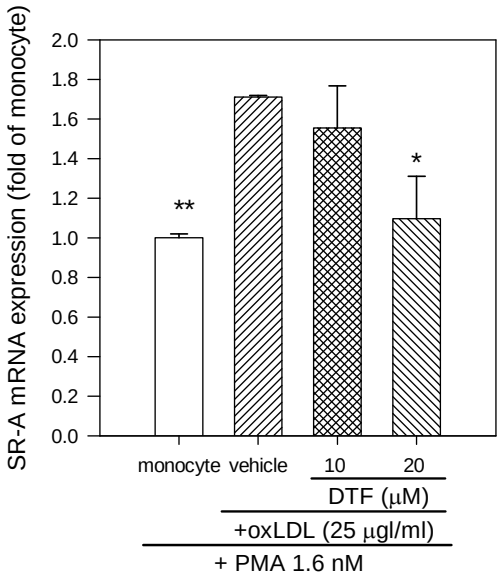
SR-A mRNA expression (fold of monocyte)
2.0
1.8
1.6
1.4
1.2
1.0
0.8
0.6
0.4
0.2
0.0
**
*
monocyte
vehicle
10
20
DTF (μM)
+oxLDL (25 μgl/ml)
+ PMA 1.6 nM

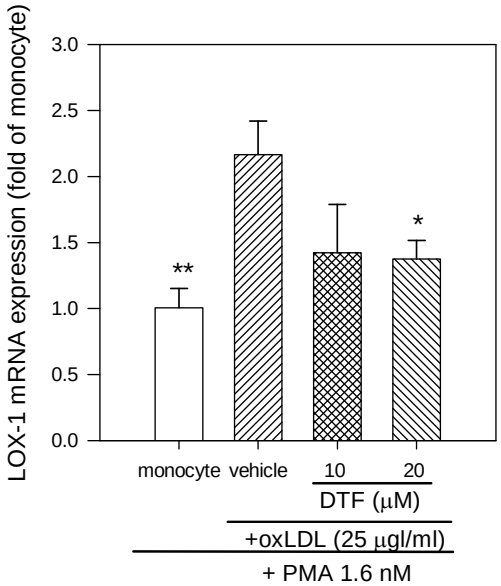
LOX-1 mRNA expression (fold of monocyte)
3.0
2.5
2.0
1.5
1.0
0.5
0.0
**
*
monocyte
vehicle
10
20
DTF (μM)
+oxLDL (25 μgl/ml)
+ PMA 1.6 nM

(Figure 4)

A

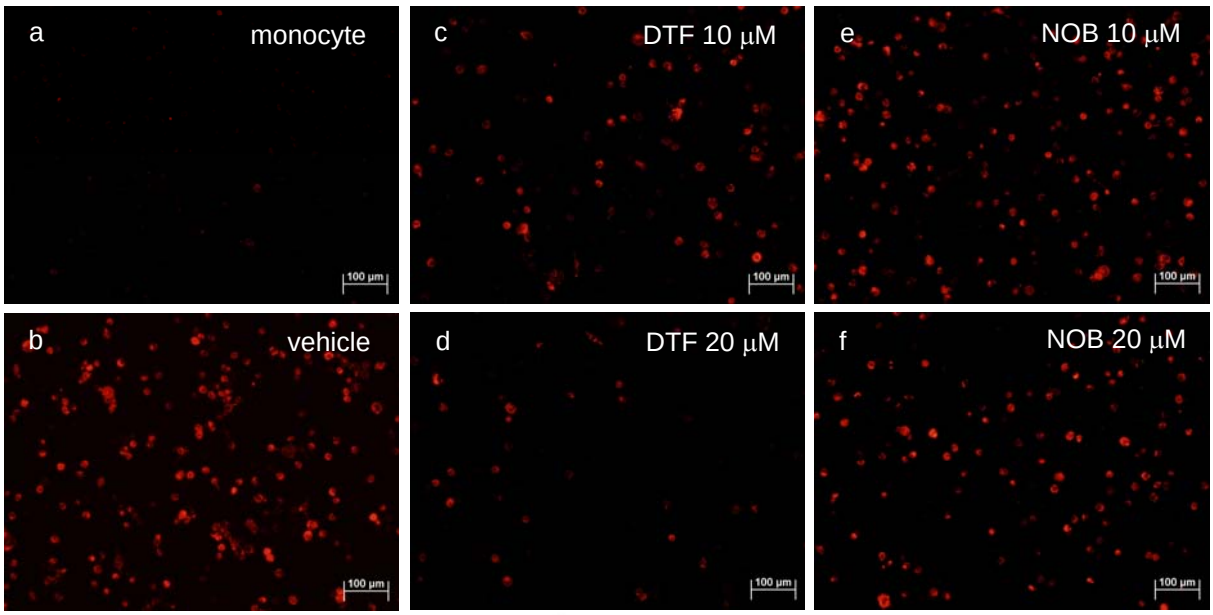

B

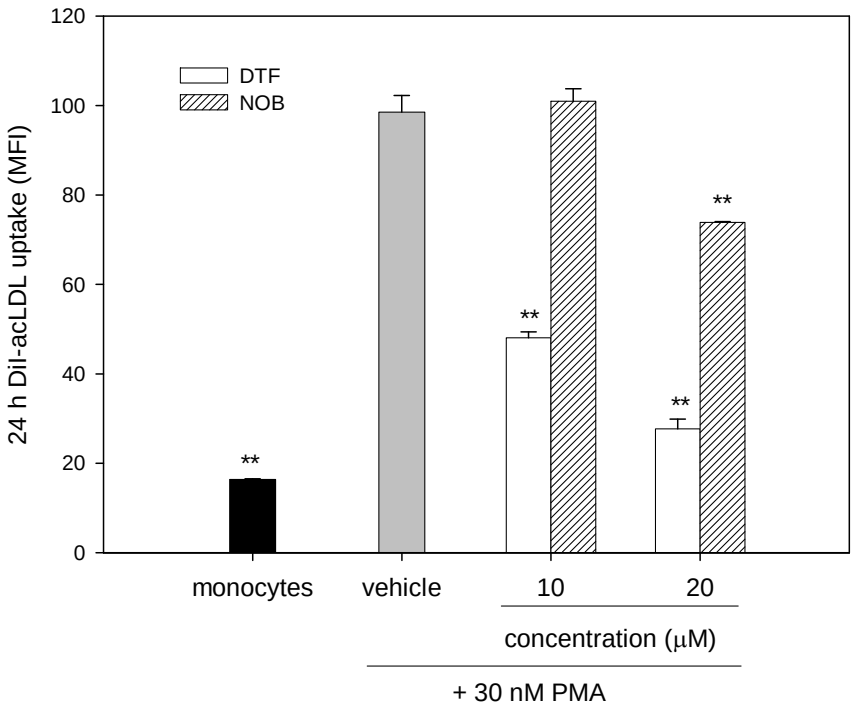

(Figure 5AB)

C

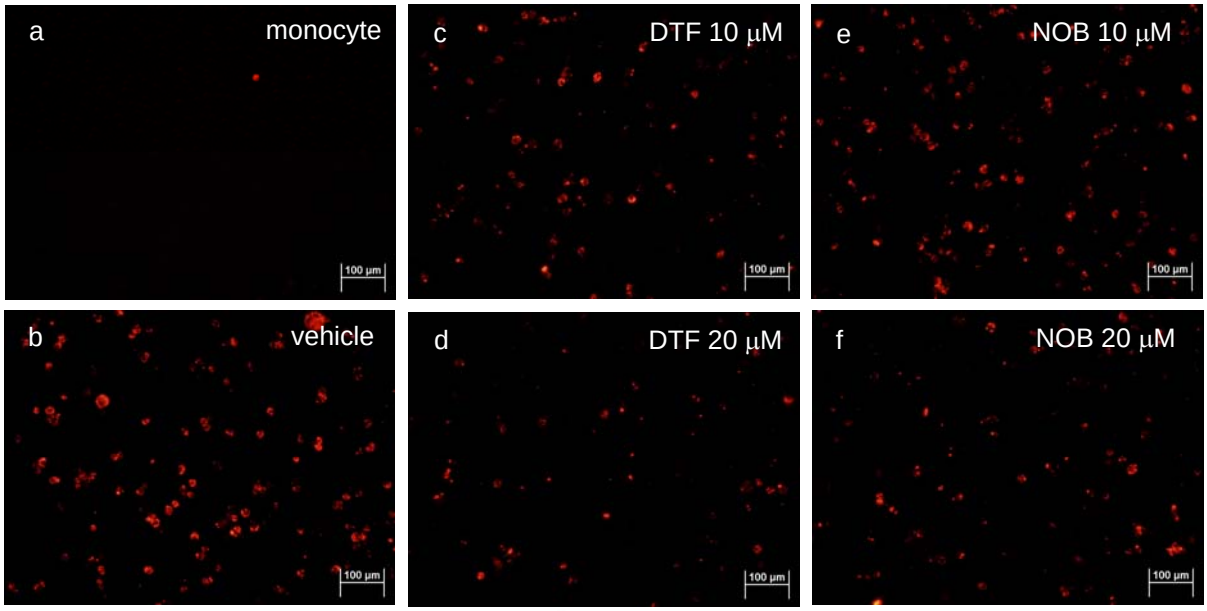

D

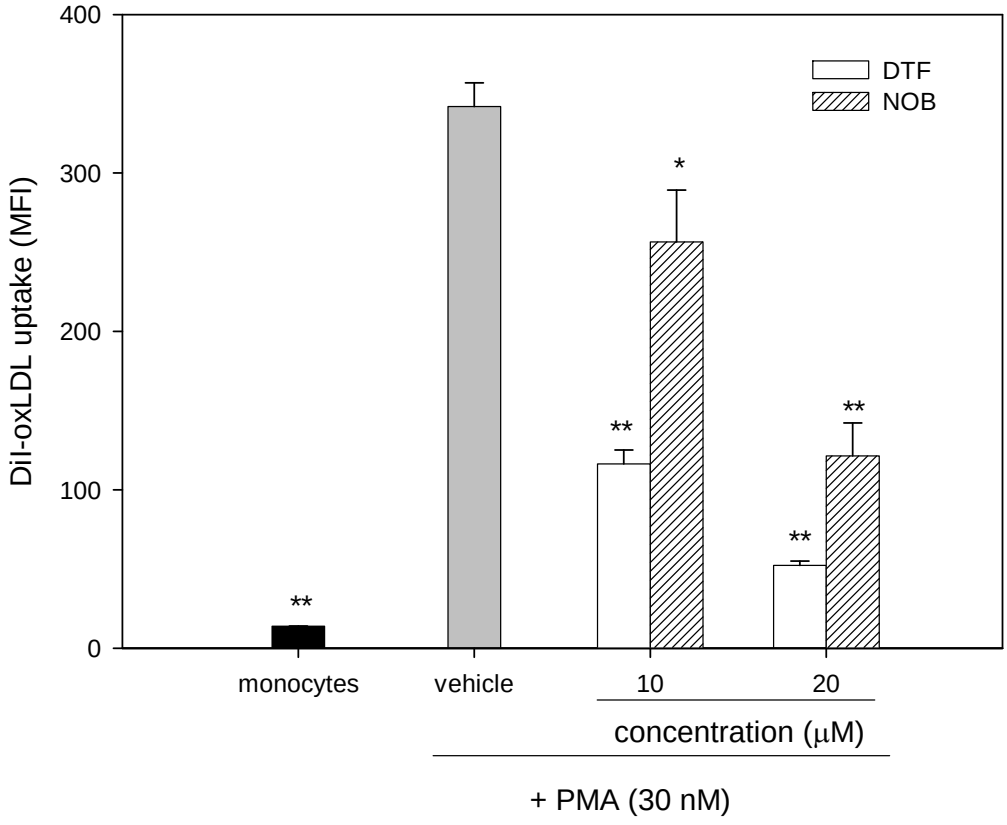

(Figure 5CD)

A

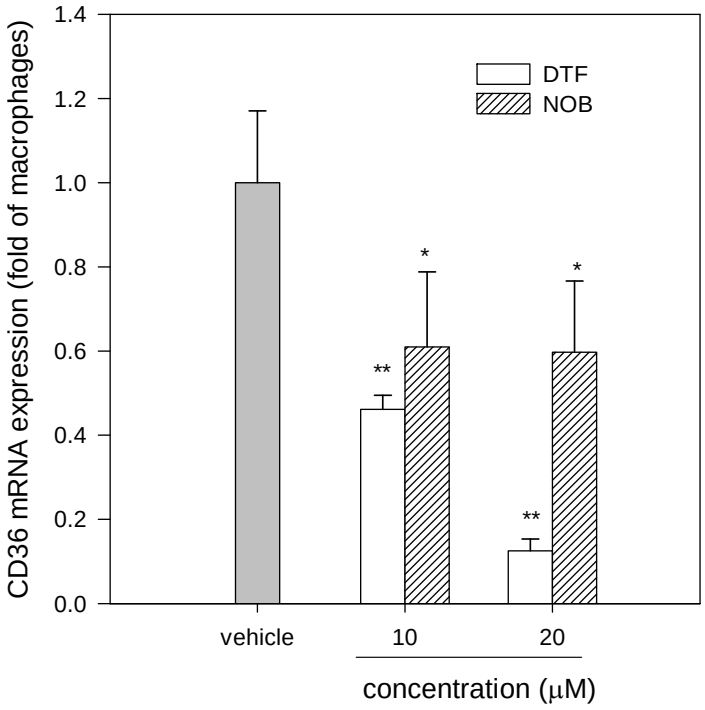

B

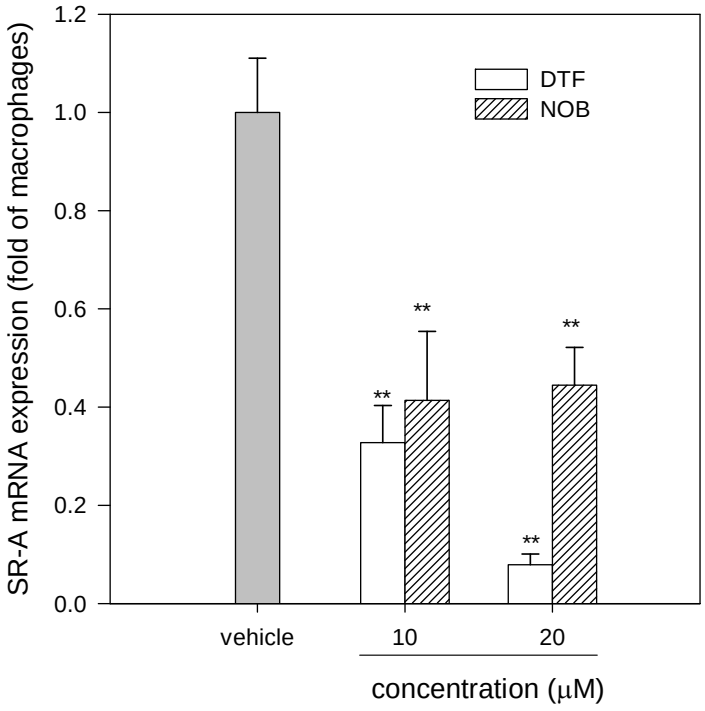

(Figure 6 A and B)

C

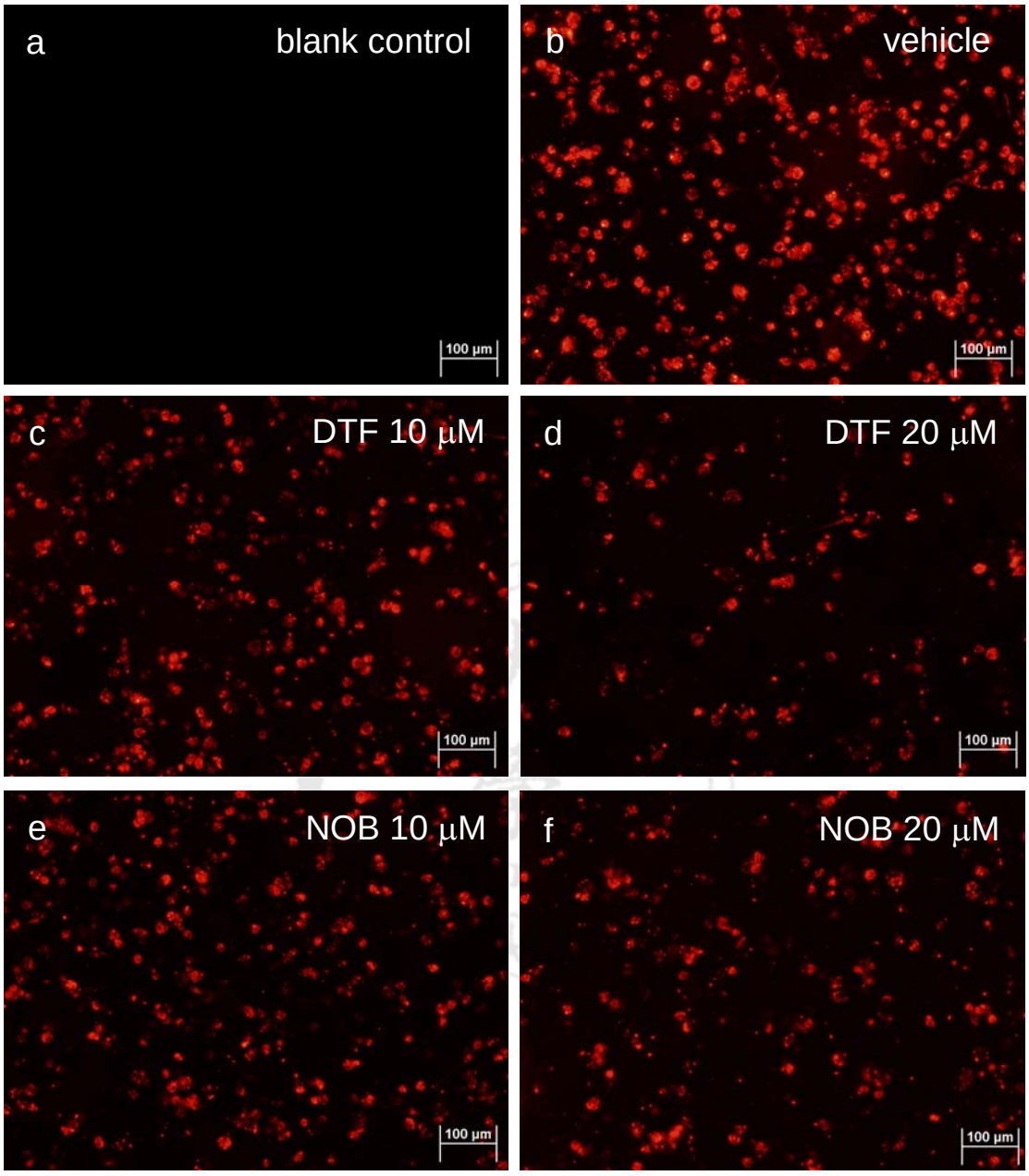
a
blank control
100 μm
b
vehicle
100 μm
c
DTF 10 μM
100 μm
d
DTF 20 μM
100 μm
e
NOB 10 μM
100 μm
f
NOB 20 μM
100 μm

(Figure 6 C)

D

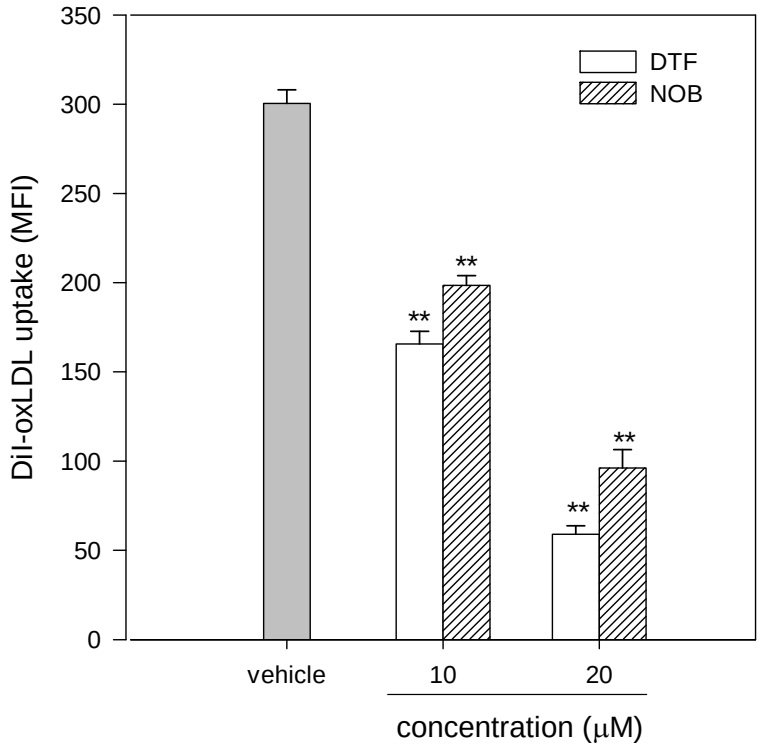

E

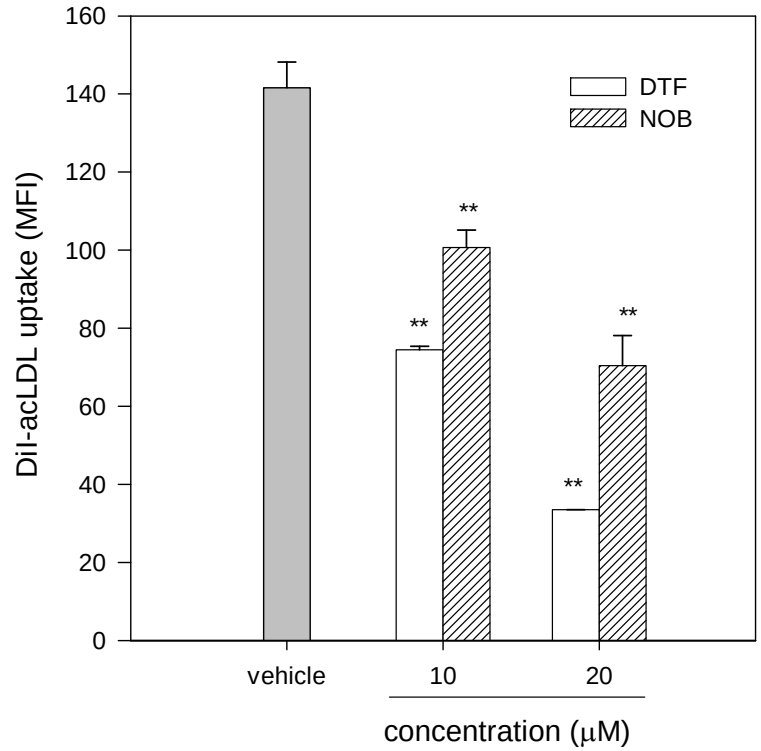

(Figure 6 D and E)

[1] P. Libby, Inflammation in atherosclerosis, Nature 420 (2002) 868-874.
[2] M. Kaplan, M. Aviram, Oxidized low density lipoprotein: atherogenic and proinflammatory characteristics during macrophage foam cell formation. An inhibitory role for nutritional antioxidants and serum paraoxonase, Clin. Chem. Lab. Med. 37 (1999) 777-787.
[3] R. Ross, Atherosclerosis--an inflammatory disease, N. Engl. J. Med. 340 (1999) 115-126.
[4] Y. Yamada, T. Doi, T. Hamakubo, T. Kodama, Scavenger receptor family proteins: roles for atherosclerosis, host defence and disorders of the central nervous system, Cell. Mol. Life Sci. 54 (1998) 628-640.
[5] W.J. de Villiers, E.J. Smart, Macrophage scavenger receptors and foam cell formation, J. Leukoc. Biol. 66 (1999) 740-746.
[6] G. Endemann, L.W. Stanton, K.S. Madden, C.M. Bryant, R.T. White, A.A. Protter, CD36 is a receptor for oxidized low density lipoprotein, J Biol Chem 268 (1993) 11811-11816.
[7] Y. Zeng, N. Tao, K.N. Chung, J.E. Heuser, D.M. Lublin, Endocytosis of oxidized low density lipoprotein through scavenger receptor CD36 utilizes a lipid raft pathway that does not require caveolin-1, J. Biol. Chem. 278 (2003) 45931-45936.
[8] A. Nakata, Y. Nakagawa, M. Nishida, S. Nozaki, J. Miyagawa, T. Nakagawa, R. Tamura, K. Matsumoto, K. Kameda-Takemura, S. Yamashita, Y. Matsuzawa, CD36, a novel receptor for oxidized low-density lipoproteins, is highly expressed on lipid-laden macrophages in human atherosclerotic aorta, Arterioscler Thromb Vasc Biol 19 (1999) 1333-1339.
[9] D.P. Hajjar, M.E. Haberland, Lipoprotein trafficking in vascular cells. Molecular Trojan horses and cellular saboteurs, J. Biol. Chem. 272 (1997) 22975-22978.
[10] J. Han, D.P. Hajjar, M. Febbraio, A.C. Nicholson, Native and modified low density lipoproteins increase the functional expression of the macrophage class B scavenger receptor, CD36, J. Biol. Chem. 272 (1997) 21654-21659.
[11] N. Platt, S. Gordon, Is the class A macrophage scavenger receptor (SR-A) multifunctional? - The mouse's tale, J. Clin. Invest. 108 (2001) 649-654.
[12] N. Kume, T. Murase, H. Moriwaki, T. Aoyama, T. Sawamura, T. Masaki, T. Kita, Inducible expression of lectin-like oxidized LDL receptor-1 in vascular endothelial cells, Circ. Res. 83 (1998) 322-327.
[13] H. Kataoka, N. Kume, S. Miyamoto, M. Minami, H. Moriwaki, T. Murase, T. Sawamura, T. Masaki, N. Hashimoto, T. Kita, Expression of lectinlike

oxidized low-density lipoprotein receptor-1 in human atherosclerotic lesions, Circulation 99 (1999) 3110-3117.

[14] H. Moriwaki, N. Kume, T. Sawamura, T. Aoyama, H. Hoshikawa, H. Ochi, E. Nishi, T. Masaki, T. Kita, Ligand specificity of LOX-1, a novel endothelial receptor for oxidized low density lipoprotein, Arterioscler. Thromb. Vasc. Biol. 18 (1998) 1541-1547.

[15] M. Febbraio, E.A. Podrez, J.D. Smith, D.P. Hajjar, S.L. Hazen, H.F. Hoff, K. Sharma, R.L. Silverstein, Targeted disruption of the class B scavenger receptor CD36 protects against atherosclerotic lesion development in mice, J. Clin. Invest. 105 (2000) 1049-1056.

[16] H. Suzuki, Y. Kurihara, M. Takeya, N. Kamada, M. Kataoka, K. Jishage, O. Ueda, H. Sakaguchi, T. Higashi, T. Suzuki, Y. Takashima, Y. Kawabe, O. Cynshi, Y. Wada, M. Honda, H. Kurihara, H. Aburatani, T. Doi, A. Matsumoto, S. Azuma, T. Noda, Y. Toyoda, H. Itakura, Y. Yazaki, T. Kodama, et al., A role for macrophage scavenger receptors in atherosclerosis and susceptibility to infection, Nature 386 (1997) 292-296.

[17] V.R. Babaev, L.A. Gleaves, K.J. Carter, H. Suzuki, T. Kodama, S. Fazio, M.F. Linton, Reduced atherosclerotic lesions in mice deficient for total or macrophage-specific expression of scavenger receptor-A, Arterioscler. Thromb. Vasc. Biol. 20 (2000) 2593-2599.

[18] H. Sakaguchi, M. Takeya, H. Suzuki, H. Hakamata, T. Kodama, S. Horiuchi, S. Gordon, L.J. van der Laan, G. Kraal, S. Ishibashi, N. Kitamura, K. Takahashi, Role of macrophage scavenger receptors in diet-induced atherosclerosis in mice, Lab. Invest. 78 (1998) 423-434.

[19] J.L. Mehta, N. Sanada, C.P. Hu, J. Chen, A. Dandapat, F. Sugawara, H. Satoh, K. Inoue, Y. Kawase, K. Jishage, H. Suzuki, M. Takeya, L. Schnackenberg, R. Beger, P.L. Hermonat, M. Thomas, T. Sawamura, Deletion of LOX-1 reduces atherogenesis in LDLR knockout mice fed high cholesterol diet, Circ. Res. 100 (2007) 1634-1642.

[20] C. Hu, J. Chen, A. Dandapat, Y. Fujita, N. Inoue, Y. Kawase, K. Jishage, H. Suzuki, D. Li, P.L. Hermonat, T. Sawamura, J.L. Mehta, LOX-1 abrogation reduces myocardial ischemia-reperfusion injury in mice, J. Mol. Cell. Cardiol. 44 (2008) 76-83.

[21] M. Aviram, Macrophage foam cell formation during early atherogenesis is determined by the balance between pro-oxidants and anti-oxidants in arterial cells and blood lipoproteins, Antioxid. Redox. Signal. 1 (1999) 585-594.

[22] M.N. Diaz, B. Frei, J.A. Vita, J.F. Keaney, Jr., Antioxidants and atherosclerotic heart disease, N. Engl. J. Med. 337 (1997) 408-416.

[23] B. Fuhrman, N. Volkova, R. Coleman, M. Aviram, Grape Powder Polyphenols Attenuate Atherosclerosis Development in Apolipoprotein E Deficient (E0) Mice and Reduce Macrophage Atherogenicity, J. Nutr. 135 (2005) 722-728.

[24] B. Fuhrman, M. Aviram, Anti-atherogenicity of nutritional antioxidants, IDrugs 4 (2001) 82-92.

[25] B. Fuhrman, M. Aviram, Flavonoids protect LDL from oxidation and attenuate atherosclerosis, Curr. Opin. Lipidol. 12 (2001) 41-48.

[26] A. Munteanu, J.M. Zingg, R. Ricciarelli, A. Azzi, CD36 overexpression in ritonavir-treated THP-1 cells is reversed by alpha-tocopherol, Free Radic. Biol. Med. 38 (2005) 1047-1056.

[27] Y. Kawai, T. Nishikawa, Y. Shiba, S. Saito, K. Murota, N. Shibata, M. Kobayashi, M. Kanayama, K. Uchida, J. Terao, Macrophage as a target of quercetin glucuronides in human atherosclerotic arteries: implication in the anti-atherosclerotic mechanism of dietary flavonoids, J. Biol. Chem. 283 (2008) 9424-9434.

[28] T.W. Lian, L. Wang, Y.H. Lo, I.J. Huang, M.J. Wu, Fisetin, morin and myricetin attenuate CD36 expression and oxLDL uptake in U937-derived macrophages, Biochim. Biophys. Acta 1781 (2008) 601-609.

[29] A. Munteanu, M. Taddei, I. Tamburini, E. Bergamini, A. Azzi, J.M. Zingg, Antagonistic effects of oxidized low density lipoprotein and alpha-tocopherol on CD36 scavenger receptor expression in monocytes: involvement of protein kinase B and peroxisome proliferator-activated receptor-gamma, J. Biol. Chem. 281 (2006) 6489-6497.

[30] S. Devaraj, I. Hugou, I. Jialal, Alpha-tocopherol decreases CD36 expression in human monocyte-derived macrophages, J. Lipid Res. 42 (2001) 521-527.

[31] E.M. Kurowska, J.A. Manthey, Hypolipidemic effects and absorption of citrus polymethoxylated flavones in hamsters with diet-induced hypercholesterolemia, J. Agric. Food Chem. 52 (2004) 2879-2886.

[32] J.M. Roza, Z. Xian-Liu, N. Guthrie, Effect of citrus flavonoids and tocotrienols on serum cholesterol levels in hypercholesterolemic subjects, Altern. Ther. Health Med. 13 (2007) 44-48.

[33] L.J. Wilcox, N.M. Borradaile, L.E. de Dreu, M.W. Huff, Secretion of hepatocyte apoB is inhibited by the flavonoids, naringenin and hesperetin, via reduced activity and expression of ACAT2 and MTP, J. Lipid Res. 42 (2001) 725-734.

[34] B. Morin, L.A. Nichols, K.M. Zalasky, J.W. Davis, J.A. Manthey, L.J. Holland, The Citrus Flavonoids Hesperetin and Nobiletin Differentially Regulate Low Density Lipoprotein Receptor Gene Transcription in HepG2

Liver Cells, J. Nutr. 138 (2008) 1274-1281.

[35] A. Eguchi, A. Murakami, H. Ohigashi, Nobiletin, a citrus flavonoid, suppresses phorbol ester-induced expression of multiple scavenger receptor genes in THP-1 human monocytic cells, FEBS Lett. 580 (2006) 3321-3328.

[36] S.C. Whitman, E.M. Kurowska, J.A. Manthey, A. Daugherty, Nobiletin, a citrus flavonoid isolated from tangerines, selectively inhibits class A scavenger receptor-mediated metabolism of acetylated LDL by mouse macrophages, Atherosclerosis 178 (2005) 25-32.

[37] C.S. Lai, S. Li, C.Y. Chai, C.Y. Lo, S. Dushenkov, C.T. Ho, M.H. Pan, Y.J. Wang, Anti-inflammatory and antitumor promotional effects of a novel urinary metabolite, 3',4'-didemethylnobiletin, derived from nobiletin, Carcinogenesis 29 (2008) 2415-2424.

[38] S. Li, S. Sang, M.H. Pan, C.S. Lai, C.Y. Lo, C.S. Yang, C.T. Ho, Anti-inflammatory property of the urinary metabolites of nobiletin in mouse, Bioorg. Med. Chem. Lett. 17 (2007) 5177-5181.

[39] A. Eguchi, A. Murakami, S. Li, C.T. Ho, H. Ohigashi, Suppressive effects of demethylated metabolites of nobiletin on phorbol ester-induced expression of scavenger receptor genes in THP-1 human monocytic cells, Biofactors 31 (2007) 107-116.

[40] H. Esterbauer, G. Striegl, H. Puhl, M. Rotheneder, Continuous monitoring of in vitro oxidation of human low density lipoprotein, Free Radic. Res. Commun. 6 (1989) 67-75.

[41] G. Knipping, M. Rotheneder, G. Striegl, H. Esterbauer, Antioxidants and resistance against oxidation of porcine LDL subfractions, J. Lipid Res. 31 (1990) 1965-1972.

[42] L. Lanningham-Foster, C. Chen, D.S. Chance, G. Loo, Grape extract inhibits lipid peroxidation of human low density lipoprotein, Biol. Pharm. Bull. 18 (1995) 1347-1351.

[43] A.M. Gotto, Jr., H.J. Pownall, R.J. Havel, Introduction to the plasma lipoproteins, Methods Enzymol 128 (1986) 3-41.

[44] M.M. Bradford, A rapid and sensitive method for the quantitation of microgram quantities of protein utilizing the principle of protein-dye binding, Anal Biochem 72 (1976) 248-254.

[45] H.A. Kleinveld, H.L. Hak-Lemmers, A.F. Stalenhoef, P.N. Demacker, Improved measurement of low-density-lipoprotein susceptibility to copper-induced oxidation: application of a short procedure for isolating low-density lipoprotein, Clin Chem 38 (1992) 2066-2072.

[46] M. Hermann, B. Gmeiner, Altered susceptibility to in vitro oxidation of LDL

in LDL complexes and LDL aggregates, Ann N Y Acad Sci 683 (1993) 363-364.

[47] B. Fuhrman, A. Partoush, N. Volkova, M. Aviram, Ox-LDL induces monocyte-to-macrophage differentiation in vivo: Possible role for the macrophage colony stimulating factor receptor (M-CSF-R), Atherosclerosis 196 (2008) 598-607.

[48] X. Wang, B. Seed, A PCR primer bank for quantitative gene expression analysis, Nucl. Acids Res. 31 (2003) e154.

[49] D. Teupser, J. Thiery, A.K. Walli, D. Seidel, Determination of LDL- and scavenger-receptor activity in adherent and non-adherent cultured cells with a new single-step fluorometric assay, Biochimica et Biophysica Acta (BBA) - Lipids and Lipid Metabolism 1303 (1996) 193-198.

[50] S.K. Basu, J.L. Goldstein, G.W. Anderson, M.S. Brown, Degradation of cationized low density lipoprotein and regulation of cholesterol metabolism in homozygous familial hypercholesterolemia fibroblasts, Proc. Natl. Acad. Sci. U. S. A. 73 (1976) 3178-3182.

[51] U.P. Steinbrecher, H.F. Zhang, M. Lougheed, Role of oxidatively modified LDL in atherosclerosis, Free Radic Biol Med 9 (1990) 155-168.

[52] P.M. Abuja, H. Esterbauer, Simulation of lipid peroxidation in low-density lipoprotein by a basic "skeleton" of reactions, Chem. Res. Toxicol. 8 (1995) 753-763.

[53] O. Ziouzenkova, A. Sevanian, P.M. Abuja, P. Ramos, H. Esterbauer, Copper can promote oxidation of LDL by markedly different mechanisms, Free Radic. Biol. Med. 24 (1998) 607-623.

[54] J. Auwerx, The human leukemia cell line, THP-1: a multifacetted model for the study of monocyte-macrophage differentiation, Experientia 47 (1991) 22-31.

[55] J. Carmichael, W.G. DeGraff, A.F. Gazdar, J.D. Minna, J.B. Mitchell, Evaluation of a tetrazolium-based semiautomated colorimetric assay: assessment of chemosensitivity testing, Cancer Res. 47 (1987) 936-942.

[56] M.A. Arnaout, Structure and function of the leukocyte adhesion molecules CD11/CD18, Blood 75 (1990) 1037-1050.

[57] V.V. Kunjathoor, M. Febbraio, E.A. Podrez, K.J. Moore, L. Andersson, S. Koehn, J.S. Rhee, R. Silverstein, H.F. Hoff, M.W. Freeman, Scavenger receptors class A-I/II and CD36 are the principal receptors responsible for the uptake of modified low density lipoprotein leading to lipid loading in macrophages, J. Biol. Chem. 277 (2002) 49982-49988.

[58] M.T. Quinn, S. Parthasarathy, L.G. Fong, D. Steinberg, Oxidatively modified

low density lipoproteins: a potential role in recruitment and retention of monocyte/macrophages during atherogenesis, Proc. Natl. Acad. Sci. U. S. A. 84 (1987) 2995-2998.

[59] J.M. Hayden, L. Brachova, K. Higgins, L. Obermiller, A. Sevanian, S. Khandrika, P.D. Reaven, Induction of monocyte differentiation and foam cell formation in vitro by 7-ketocholesterol, J. Lipid Res. 43 (2002) 26-35.

[60] J. Frostegard, J. Nilsson, A. Haegerstrand, A. Hamsten, H. Wigzell, M. Gidlund, Oxidized low density lipoprotein induces differentiation and adhesion of human monocytes and the monocytic cell line U937, Proc. Natl. Acad. Sci. U. S. A. 87 (1990) 904-908.

[61] J. Pou, A. Rebollo, N. Roglans, R.M. Sanchez, M. Vazquez-Carrera, J.C. Laguna, J. Pedro-Botet, M. Alegret, Ritonavir increases CD36, ABCA1 and CYP27 expression in THP-1 macrophages, Exp Biol Med (Maywood) 233 (2008) 1572-1582.

[62] Y.C. Tu, T.W. Lian, J.H. Yen, Z.T. Chen, M.J. Wu, Antiatherogenic effects of kaempferol and rhamnocitrin, J. Agric. Food Chem. 55 (2007) 9969-9976.

[63] M. Vinals, I. Bermudez, G. Llaverias, M. Alegret, R.M. Sanchez, M. Vazquez-Carrera, J.C. Laguna, Aspirin increases CD36, SR-BI, and ABCA1 expression in human THP-1 macrophages, Cardiovasc. Res. 66 (2005) 141-149.

[64] D. Steinberg, S. Parthasarathy, T. Carew, J. Khoo, J. Witztum, Beyond cholesterol. Modifications of lowdensity lipoprotein that increase its atherogenicity, N. Engl. J. Med. 320 (1989) 915-924.

[65] C.V. de Whalley, S.M. Rankin, J.R. Hoult, W. Jessup, D.S. Leake, Flavonoids inhibit the oxidative modification of low density lipoproteins by macrophages, Biochem Pharmacol 39 (1990) 1743-1750.

[66] M.R. Safari, N. Sheikh, Effects of flavonoids on the susceptibility of low-density lipoprotein to oxidative modification, Prostaglandins Leukot Essent Fatty Acids 69 (2003) 73-77.

[67] G.A. Naderi, S. Asgary, N. Sarraf-Zadegan, H. Shirvany, Anti-oxidant effect of flavonoids on the susceptibility of LDL oxidation, Mol Cell Biochem 246 (2003) 193-196.

[68] S. Miura, J. Watanabe, M. Sano, T. Tomita, T. Osawa, Y. Hara, I. Tomita, Effects of various natural antioxidants on the Cu(2+)-mediated oxidative modification of low density lipoprotein, Biol Pharm Bull 18 (1995) 1-4.

[69] U.P. Steinbrecher, J.L. Witztum, S. Parthasarathy, D. Steinberg, Decrease in reactive amino groups during oxidation or endothelial cell modification of LDL. Correlation with changes in receptor-mediated catabolism,

Arteriosclerosis 7 (1987) 135-143.

[70] D. Steinberg, Low density lipoprotein oxidation and its pathobiological significance, J. Biol. Chem. 272 (1997) 20963-20966.

[71] H. Esterbauer, Cytotoxicity and genotoxicity of lipid-oxidation products, Am. J. Clin. Nutr. 57 (1993) 779S-785S; discussion 785S-786S.

[72] T.T. Tuomisto, M.S. Riekkinen, H. Viita, A.-L. Levonen, S. Yl?Herttuala, Analysis of gene and protein expression during monocyte-macrophage differentiation and cholesterol loading--cDNA and protein array study, Atherosclerosis 180 (2005) 283-291.

[73] J. Zhang, W. Chu, I. Crandall, Lipoprotein binding preference of CD36 is altered by filipin treatment, Lipids Health Dis. 7 (2008) 23.

[74] D. Klein, Quantification using real-time PCR technology: applications and limitations, Trends Mol. Med. 8 (2002) 257-260.

[75] A. Munteanu, M. Taddei, I. Tamburini, E. Bergamini, A. Azzi, J.-M. Zingg, Antagonistic effects of oxLDL and alpha -tocopherol on CD36 scavenger receptor expression in monocytes; involvement of PKB and PPARgamma, J. Biol. Chem. (2006) M508799200.

[76] H. Schwende, E. Fitzke, P. Ambs, P. Dieter, Differences in the state of differentiation of THP-1 cells induced by phorbol ester and 1,25-dihydroxyvitamin D3, J. Leukoc. Biol. 59 (1996) 555-561.

[77] N. Koga, M. Matsuo, C. Ohta, K. Haraguchi, M. Matsuoka, Y. Kato, T. Ishii, M. Yano, H. Ohta, Comparative Study on Nobiletin Metabolism with Liver Microsomes from Rats, Guinea Pigs and Hamsters and Rat Cytochrome P450, Biol. Pharm. Bull. 30 (2007) 2317-2323.

嘉南藥理科技大學專題研究計畫成果報告

計畫編號：CN9803

總計畫名稱：多酚化合物活性及有效成分探討

子計畫（三）名稱:虎杖乙醇萃取物抗EB病毒主要活性成分之鑑定

執行期間：98 年 1 月 1 日至 98 年 12 月 31 日

■整合型計畫	□個別型計畫
計畫總主持人：楊朝成	計畫主持人：
子計畫主持人：一. 楊朝成 二. 吳明娟 三. 葉東柏	

中華民國 99 年 2 月 28 日

子計畫三：虎杖乙醇萃取物抗 EB 病毒主要活性成分之鑑定

主持人：生物科技系 葉東柏
共同主持人：保健營養系 林翠品

一、摘要

EB 病毒從潛伏循環再活化至溶裂循環會導致病毒顆粒的產生而使得細胞受到 EB 病毒的感染。在這個研究我們探討虎杖乙醇萃取物抑制 EB 病毒溶裂循環的主要活性成分, 結果發現虎杖乙醇萃取物(PcE)在 25 μg/ml 時，抑制 50%以上 Rta、Zta 及 EA-D 的表現，而正己烷處理之極性層分劃物[PcE(H)]在 50 μg/ml 對 EB 病毒溶裂循環蛋白質，Rta 及 EA-D 表現才有 50%的抑制能力，另外對 Zta 表現只有約 26%的抑制效果。進一步的研究顯示，乙酸乙酯分劃物(PcEE) 只需 3.1 μg/ml 對 EB 病毒溶裂循環蛋白質，Zta 及 EA-D 表現就有 50%的抑制能力。而且也發現在具有抑制 EB 病毒溶裂蛋白質表現的濃度下對細胞不會造成毒性。此外，也發現乙酸乙酯分劃物(PcEE)的大黃素含量也上升 6 倍，所以由這些結果顯示大黃素在虎杖乙醇萃取物中很可能就是扮演著抑制病毒進入溶裂循環，進而阻擋病毒再活化的主要成分。

關鍵字: Epstein-Barr 病毒；虎杖萃取物；抗病毒；細胞毒性

二、緣由與目的

EB 病毒是人類的皰疹病毒(herpesvirus)，會感染淋巴球細胞及上皮細胞[(1)]，導致傳染性單核球增多症(infectious monnucleosis)[(2)]及多種惡質病(malignant disease)包括巴克氏淋巴瘤(Burkitt's lymphoma)[(3)]、T 細胞淋巴瘤[(4)]、霍奇金氏病(Hodgkin's disease)[(5)]、胃癌(gastric cancer)[(6)]及鼻咽癌(nasopharyngeal carcinoma)[(7)]。病毒感染 B 淋巴球細胞後會進入潛伏時期(latent)[(8)]，但是當受到外在因子包括紫外線[(9)]、12-O-tetradecanoylphorbol-13-acetate (TPA)[(10)], sodium butyrate(SB)[(11)]就會由潛伏時期進入溶裂循環(lytic cycle)進行增殖作用再感染其他細胞，此作用與 EB 病毒所導致的疾病有重要的相關性。在溶裂循環時期病毒會表現兩個較早期基因(immediate-early genes)，BRLF1 及 BZLF1 它們分別可以表現轉錄因子 Rta 及 Zta[(12)]，這兩個轉錄因子可以互相作用或單獨活化其他與溶裂循環時期有關的基因表現，包括 BMRF1 及 BALF5 分別表現 diffused early antigen (EA-D)及 DNA 聚合酶(polymerase)[(13)]。換言之，如果沒有這些溶裂蛋白質的表現就無法完成溶裂循環，就可以降低發生 EB 病毒相關疾病的危險性。目前一般對皰疹病毒的治療是以 acyclovir 和 ganciclovir，這兩種是核苷酸的類似物主要抑制 DNA 聚合酶(polymerase)使病毒無法進行溶裂循環，也就無法再感染其他的細胞[(14)]。在先前研究發現虎杖根乙醇萃取物在濃度 25 μg/ml 時能夠抑制丁酸鈉 (sodium butyrate) 所誘發 EB 病毒早期基因的轉錄，影響 EB 病毒溶裂蛋白質的表現，進而抑制病毒顆粒的產生。分析虎杖根乙醇萃取物的成分，發現大黃素及白黎蘆醇在萃取物中分別佔 5.1%及 2.1%，以大黃素及白黎蘆醇探討對 EB 病毒溶裂循環的影響發現分別在 9.37 μM (2.53 μg/ml)及 55 μM (12.55 μg/ml)才有明顯抑制病毒顆粒產生的能力，使 EB 病毒早期基因的轉錄及蛋白質的表現降低，進而抑制病毒顆粒的產生。所以推測虎杖根乙醇萃取物含有抑制 EB 病毒溶裂循環，而

此作用不只藉由大黃素及白黎蘆醇的作用，可能還有其他物質參與，所以本研究將進一步純化並且鑑定虎杖乙醇萃取物內抗病毒的活性成分，研究成果將有助於開發預防鼻咽癌及胃癌的天然物，也提高虎杖的經濟效益及利用率。

三、材料與方法

(一)、虎杖根乙醇萃取物及分劃物的製備

將虎杖根放置烘箱以 37℃乾燥五天讓水分完全去除，之後使用粉碎機打成粉末。秤取 10 克的粉末以 100 ml 95% 乙醇在 80℃水浴機迴流 2 小時，經由紗布初過濾後，再經由 6500 xg 離心 10 分鐘去除雜質收集上清液(這些步驟重複二次)，接著將三次所收集的上清液進行真空減壓濃縮 (EYELA rotary evaporator N-100) 去除有機溶劑，以冷凍乾燥得到虎杖根乙醇萃取物粉末(PcE)備用 (圖一 A)，萃取率為 21.6%。10 克虎杖根乙醇萃取物粉末回溶於 1000 ml 乙醇 (1:100, W/V)，再加入 100 ml 的水及 1000 ml 正己烷進行分相萃取，經分層後取極性層的部分再重複以 1000 ml 正己烷進行分相萃取，經分層取極性層的部分進行真空減壓濃縮及冷凍乾燥得到正己烷處理之極性層分劃物[PcE(H)]粉末；萃取率為 17.8%。此外也將減壓濃縮至去除正己烷處理之極性層分劃物的濃縮物溶於水總量為 100 ml 並且加入等量的乙酸乙酯進行分相萃取，靜置分層後取乙酸乙酯層進行減壓濃縮及冷凍乾燥得到乙酸乙酯分劃物(PcEE)粉末，萃取率為 4.4%。取部分粉末溶於 DMSO (最終濃度 0.1%)進行活性分析。

(二)、虎杖根乙醇萃取物內活性成份之逆相式高效液相色層分析

將虎杖根乙醇萃取物(PcE)，正己烷處理之極性層分劃物[PcE(H)]及乙酸乙酯分劃物(PcEE)以高效液相色層分析，所用的條件：逆相式，C18 (250 × 8 mm)的分離管，移動相為甲醇及水 (methanol: 0–15 min, 30–50%; 15–35 min, 50–90%; 35–45 min, 95%)，流速為 1 ml/min，檢測器設定值為 280 nm，此外乙酸乙酯分劃物(PcEE)經由逆相式高效液相色層分析，接著收集不同時間點出現的波峰，將收集液分成三群(F1-F3) (F1=0~20.96，F2=20.96~33.28，F3=33.28~45)，進一步將收集液減壓濃縮去除有機溶劑，以真空冷凍乾燥所得粉末定量溶於 DMSO 測量抗病毒生物活性。

(三)、抗病毒生物活性分析

抗病毒活性分析，將 P3HR1 細胞 (6×10^5 cell/ml) 放置在 5% CO_2 、37℃培養 24 小時後，再加入 SB (Sodium butyrate)誘導細胞進入溶裂循環前一小時加入虎杖根乙醇萃取物(PcE)，正己烷處理之極性層分劃物[PcE(H)]及乙酸乙酯分劃物(PcEE)培養 24 小時後收集細胞，再以 lysis buffer 溶解細胞，經過離心取得上清液蛋白質，進一步利用西方墨點法來分析 EB 病毒溶裂蛋白質 Rta, Zta 及 EA-D 的表現並且以影像分析軟體(VisionWorksLS)掃描影像強度進行數據分析，以β-actn 相對比較換算 Rta，Zta 及 EA-D 相對表現量。

(四)、細胞毒性分析

將 1×10^5 cell/ml 的 P3HR1 細胞以含有 10% 胎牛血清及 1% 抗生素(penicillin-G & streptomycin)的 HyQ RPMI 1640 培養基，在 5% CO_2 、37℃培養 24 小時後，分別添加

不同濃度的虎杖根乙醇萃取物(PcE)，正己烷處理之極性層分劃物[PcE(H)]及乙酸乙酯分劃物(PcEE)，培養 24 小時後，加入 0.5 mg/ml 的 MTT 試劑，置於 5% CO_2 、37℃反應作用 4 小時，接著離心收集細胞去除培養基，將收集的細胞加入 1 ml 100% DMSO 溶出暗藍色沉澱物，測定A_{492}。

相對細胞生長存活率(%)＝(A_{492}treatment / A_{492}control)× 100%

四、結果

(一)、虎杖根乙醇萃取物及分劃物內活性成份之逆相式高效液相色層分析

將虎杖根乙醇萃取物(PcE)，正己烷處理之極性層分劃物[PcE(H)]，乙酸乙酯分劃物(PcEE)及 PcEE 乙酸乙酯分離物 F1- F3 以高效液相色層分析，發現各萃取物及分劃物所含大黃素的純度分別為 5.1%，5.6%，23.1%，0.3%，0.4%及 93.4%, ；所含白黎蘆醇的醇度分別為 2.1%，2.5%，5%，10.5%，0%及 0.02%（圖二）。

（二）、虎杖根乙醇萃取物及分劃物對 EB 病毒溶裂蛋白質的影響

EB病毒感染B細胞後即進入潛伏時期，當受到紫外光或是TPA、SB等誘導，便會促使Rta及Zta轉錄因子的表現，進而使EB病毒走向溶裂循環。這兩個轉錄因子會活化BMRF1基因產生EA-D蛋白質，而增加病毒聚合酶效能，使病毒大量的複製。所以如果虎杖根乙醇萃取物或分劃物能夠抑制這些蛋白質的表現，就可以抑制EB病毒走向溶裂循環。首先培養P3HR1細胞 (6×10^5/ml)，加入不同濃度的虎杖根乙醇萃取物(PcE)，正己烷處理之極性層分劃物[PcE(H)]及乙酸乙酯分劃物(PcEE)，接著加入SB，經過24小時培養，將細胞收集並打破，利用西方墨點法偵測細胞中Rta、Zta及EA-D蛋白質的表現。結果顯示PcE在濃度12.5 mg/ml對EB病毒溶裂循環蛋白質，Rta，Zta及EA-D的表現就有明顯抑制。在25 μg/ml時，抑制50%以上Rta、Zta及EA-D的表現(圖三A)。正己烷處理之極性層分劃物[PcE(H)]在25 μg/ml對EB病毒溶裂循環蛋白質，Rta，Zta及EA-D的表現已有明顯抑制；在50 μg/ml對EB病毒溶裂循環蛋白質，Rta及EA-D的表現則有50%的抑制能力，但是對Zta的表現卻只有約26%的抑制效果(圖三B)。乙酸乙酯分劃物(PcEE)在3.1 μg/ml就對EB病毒溶裂循環蛋白質，Zta及EA-D的表現有50%抑制能力，但是對Rta蛋白質的表現卻只有22%的抑制能力(圖三C)。

(三)、虎杖根乙醇萃取物及分劃物對P3HR1細胞的毒性

將不同濃度的虎杖根乙醇萃取物(PcE)，正己烷處理之極性層分劃物[PcE(H)]，乙酸乙酯分劃物(PcEE)加入含有6×10^5/ml P3HR1細胞的培養液中，培養24小時後，利用MTT方法來測定這些樣品對於P3HR1細胞是否有毒性。結果顯示，PcE在25 μg/ml濃度以下對對P3HR1細胞存活率不會影響，但是當濃度上升至50 μg/ml時會影響細胞存活率約毒殺15%的細胞，至100 μg/ml約毒殺29%的細胞數(圖四A)。正己烷處理之極性層分劃物[PcE(H)]在50 μg/ml濃度以下對對P3HR1細胞存活率不會影響，但是當濃度上升至100 μg/ml時會影響細胞存活率約毒殺21%的細胞。而乙酸乙酯分劃物(PcEE) 在12.5 μg/ml濃度以下對P3HR1細胞存活率不會影響，當濃度為25 μg/ml時，其細胞存活率約 56%左右(圖四C)。

五、討論

皰疹病毒感染所導致的臨床症狀有唇皰疹(cold sores)，生殖器疹(genital herps)，水痘(chicken pox)及感染性單核球增多症(infectious mononucleosis)都和病毒的再活化有關。因此一般抗皰疹病毒的藥劑，如 acyclovir 和 ganciclovir 是核苷酸的類似物抑制皰疹的 DNA 聚合酶及病毒溶裂循環的複製。早期的研究證明 EB 病毒顆粒是由 B 淋巴球細胞產生傾向再去感染上皮細胞。因此在 B 淋巴球細胞中的 EB 病毒溶裂循環的再活化是導致上皮細胞癌，如鼻咽癌(nasopharyngeal carcinoma; NPC)重要癌化的步驟。因此篩選抑制溶裂循環的新物質是可以治療與 EB 病毒感染有關的疾病。

本研究發現 PcE 在 25 μg/ml 時，抑制 50%以上 Rta、Zta 及 EA-D 的表現，而正己烷處理之極性層分劃物[PcE(H)]在 50 μg/ml 時對 EB 病毒溶裂循環蛋白質，Rta 及 EA-D 表現才有 50%抑制能力，而對 Zta 表現只有約 26%的抑制效果。本研究進一步的研究發現，乙酸乙酯分劃物(PcEE) 只需 3.1 μg/ml 就對 EB 病毒溶裂循環蛋白質，Zta 及 EA-D 表現有 50%的抑制能力。而且也發現具有抑制 EB 病毒溶裂蛋白質表現的濃度對細胞不會造成毒性。所以，本研究確認了虎杖乙醇萃取物及分劃物具有抑制病毒進入溶裂循環，阻擋病毒的再活化的效果。此外，乙酸乙酯分劃物(PcEE)的大黃素含量上升 6 倍，而抑制 EB 病毒溶裂循環蛋白質表現所需的濃度也由 25 μg/ml 降至 3.1 μg/ml，由這些結果顯示大黃素在虎杖乙醇萃取物中應是扮演抑制病毒進入溶裂循環，阻擋病毒再活化的主要成分。

本研究的成果與原計畫之設定相符，且達預期目標的百分之八十以上。這個研究將有助於了解虎杖乙醇萃取物抗 EB 病毒的主要成分，如此將有利於抗病毒試劑的開發。這個研究也達成一位生物科技系碩士生及數位專題生在藥草純化及抗病毒研究技術的訓練目標。

六、參考文獻

1. Roizman, B.; Carmichael, L. E.; Deinhardt, F.; de-The, G.; Nahmias, A. J.; Plowright, W.; Rapp, F.; Sheldrick, P.; Takahashi, M.; Wolf, K., Herpesviridae. Definition, provisional nomenclature, and taxonomy. The Herpesvirus Study Group, the International Committee on Taxonomy of Viruses. Intervirology 1981;16:201-17.
2. Niedobitek, G.; Hamilton-Dutoit, S.; Herbst, H.; Finn, T.; Vetner, M.; Pallesen, G.; Stein, H., Identification of Epstein-Barr virus-infected cells in tonsils of acute infectious mononucleosis by in situ hybridization. Hum Pathol 1989;20:796-9.
3. Magrath, I.; Jain, V.; Bhatia, K., Epstein-Barr virus and Burkitt's lymphoma. Semin Cancer Biol 1992;3:285-95.
4. Jones, J. F.; Shurin, S.; Abramowsky, C.; Tubbs, R. R.; Sciotto, C. G.; Wahl, R.; Sands, J.; Gottman, D.; Katz, B. Z.; Sklar, J., T-cell lymphomas containing Epstein-Barr viral DNA in patients with chronic Epstein-Barr virus infections. N Engl J Med 1988;318:733-41.
5. Weiss, L. M.; Movahed, L. A.; Warnke, R. A.; Sklar, J., Detection of Epstein-Barr viral genomes in Reed-Sternberg cells of Hodgkin's disease. N Engl J Med 1989;320:502-6.
6. Shibata, D.; Weiss, L. M., Epstein-Barr virus-associated gastric adenocarcinoma. Am J Pathol 1992;140:769-74.
7. zur Hausen, H.; Schulte-Holthausen, H.; Klein, G.; Henle, W.; Henle, G.; Clifford, P.; Santesson, L., EBV DNA in biopsies of Burkitt tumours and anaplastic carcinomas of the nasopharynx. Nature 1970;228:1056-8.
8. Lindahl, T.; Adams, A.; Bjursell, G.; Bornkamm, G. W.; Kaschka-Dierich, C.; Jehn, U., Covalently closed circular duplex DNA of Epstein-Barr virus in a human lymphoid cell line. J Mol Biol 1976;102:511-30.
9. Miller, G., The switch between latency and replication of Epstein-Barr virus. J Infect Dis 1990;161:833-44.
10. zur Hausen, H.; O'Neill, F. J.; Freese, U. K.; Hecker, E., Persisting oncogenic herpesvirus induced by the tumour promotor TPA. Nature 1978;272:373-5.
11. Luka, J.; Kallin, B.; Klein, G., Induction of the Epstein-Barr virus (EBV) cycle in latently infected cells by n-butyrate. Virology 1979;94:228-31.
12. Giot, J. F.; Mikaelian, I.; Buisson, M.; Manet, E.; Joab, I.; Nicolas, J. C.; Sergeant, A., Transcriptional interference between the EBV transcription factors EB1 and R: both DNA-binding and activation domains of EB1 are required. Nucleic Acids Res 1991;19:1251-8.
13. Fixman, E. D.; Hayward, G. S.; Hayward, S. D., trans-acting requirements for replication of Epstein-Barr virus ori-Lyt. J Virol 1992;66:5030-9.
14. Feederle, R.; Kost, M.; Baumann, M.; Janz, A.; Drouet, E.; Hammerschmidt, W.; Delecluse, H. J., The Epstein-Barr virus lytic program is controlled by the co-operative functions of two transactivators. Embo J 2000;19:3080-9.

七、圖表

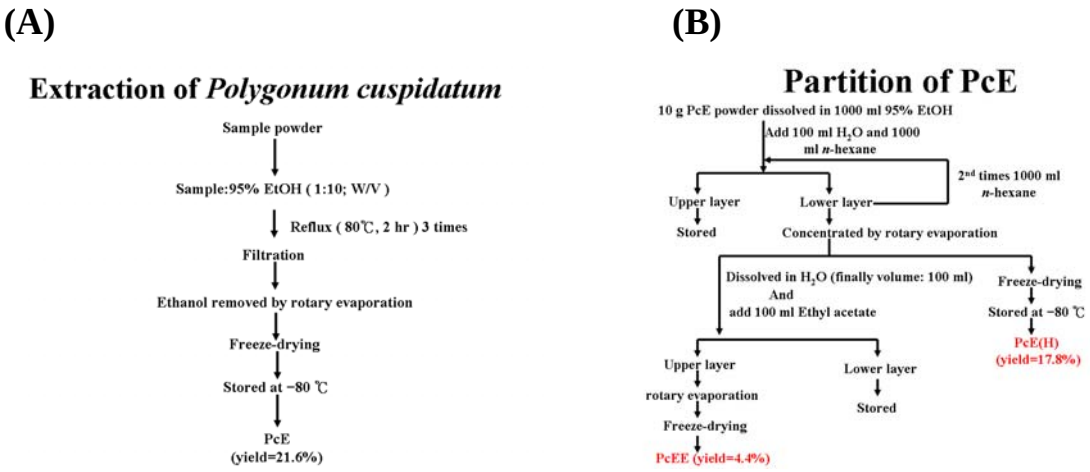

圖一、虎杖根乙醇萃取物的製備流程圖。

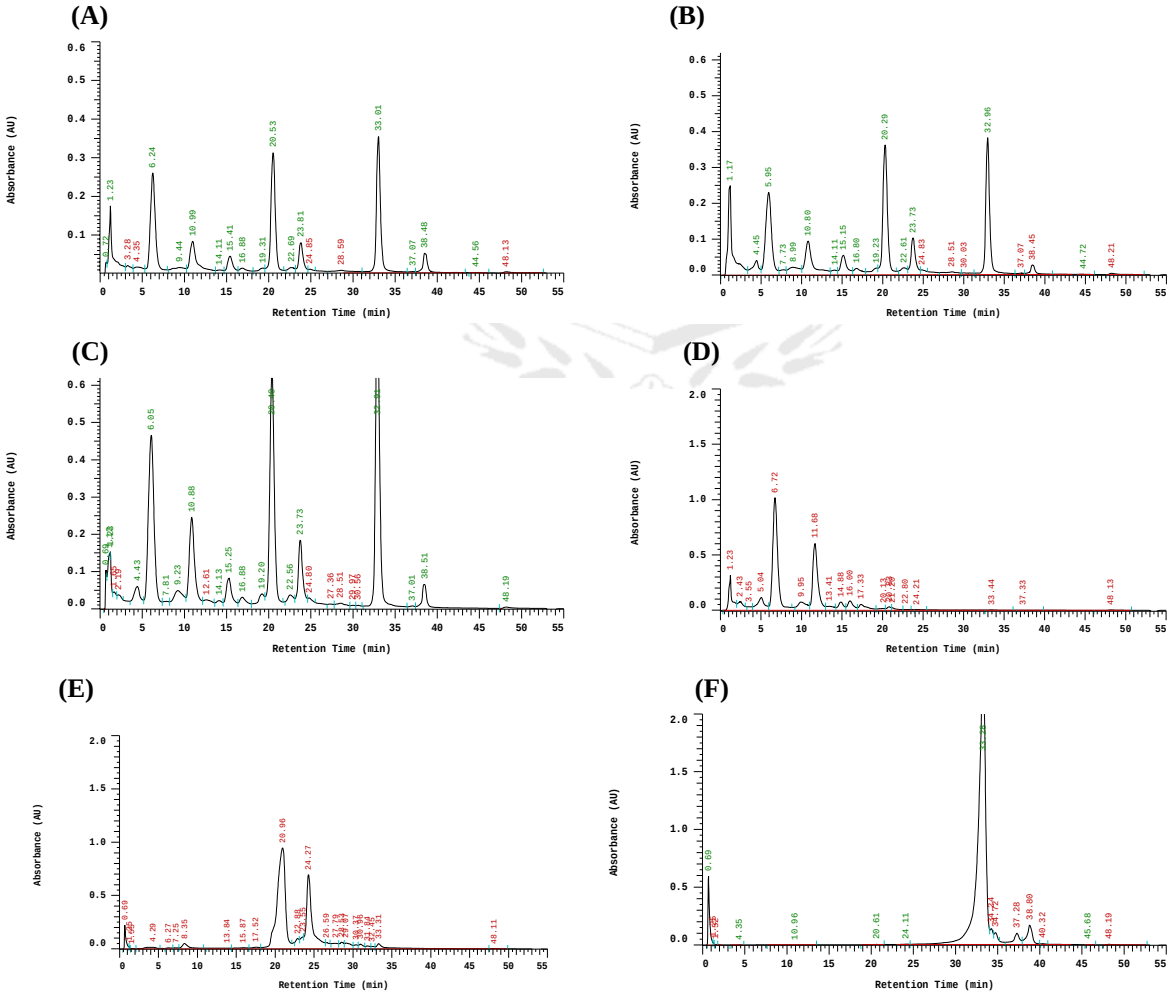

圖二、虎杖根乙醇萃取物及分劃物以 HPLC 分析之層析圖。(A)PcE，虎杖根乙醇萃取物(B) PcE(H)，正己烷處理之極性層分劃物 (C) PcEE，乙酸乙酯分劃物 (D) PcEE 乙酸乙酯分離物 F1 (E) PcEE 乙酸乙酯分離物 F2 (F) PcEE 乙酸乙酯分離物 F3。移動相: 甲醇–水(methanol: 0–15 min, 30–50%; 15–35 min, 50–90%; 35–45 min, 95%); 流速: 1.0 ml / min; 偵測的波長: 280 nm。

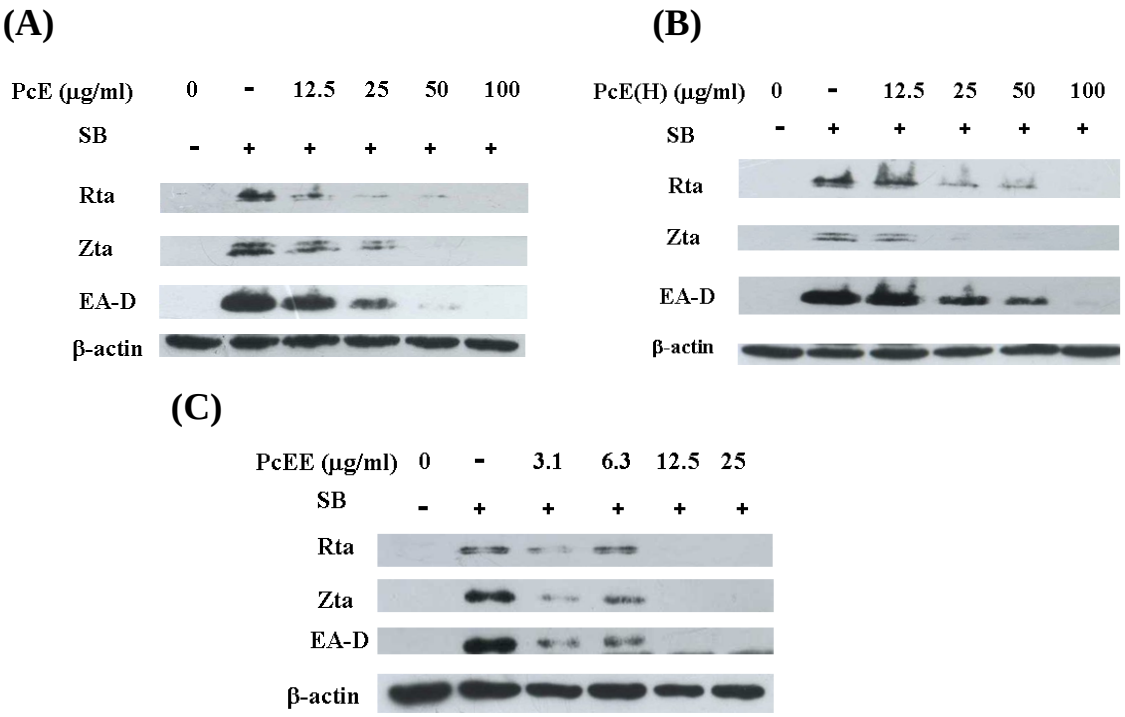

圖三、虎杖根乙醇萃取物及分劃物抑制 EB 病毒溶裂蛋白質的影響。培養含有 EB 病毒的 P3HR1 細胞 (6×10^5cell/ml)，經過 24 小時後，添加不同濃度的虎杖根之乙醇萃取物(A)、正己烷處理之極性層分劃物(B)或乙酸乙酯分劃物(C)處理，並加入誘導劑 (SB)，促使病毒走向溶裂循環，培養 24 小時後，收集細胞蛋白質。利用西方墨點法偵測 EB 病毒溶裂蛋白質 Rta、Zta、EA-D 的表現。

(A) **(B)**

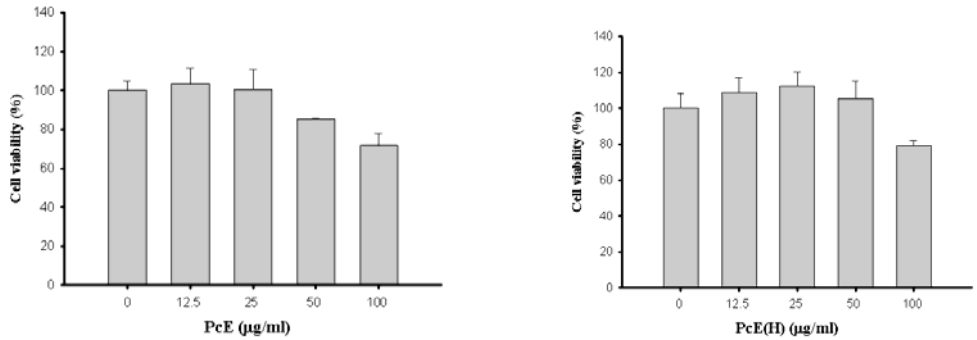

(C)

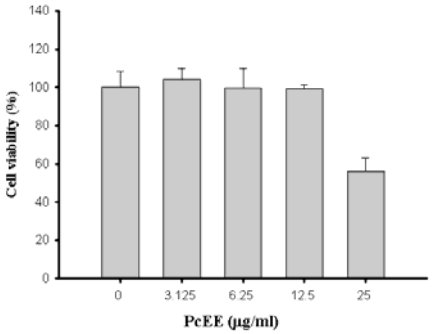

圖四、虎杖根乙醇萃取物及分劃物對於 P3HR1 細胞存活率的影響。培養含有 EB 病毒的 P3HR1 細胞 (6×10^5 cell/ml)，經過 24 小時後，添加不同濃度的虎杖根乙醇萃取物(A)、正己烷處理之極性層分劃物(B)或乙酸乙酯分劃物(C) 培養 24 小時使用 MTT 試驗法，測試不同濃度的樣品對於細胞存活率的影響。